Visual-Based Methods in Compliant Mechanism Optimization

by

Richard W. Timm

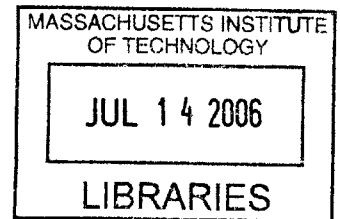B.S., Mechanical Engineering
Cornell University, 2004

Submitted to the Department of Mechanical Engineering
in Partial Fulfillment of the Requirements for the Degree of
Master of Science in Mechanical Engineering

at the

Massachusetts Institute of Technology

February 2006

Signature of Author: ...
....
Department of Mechanical Engineering
December 20, 2005

Certified by:
/...
Martin L. Culpepper III
Rockwell International Assistant Professor of Mechanical Engineering
Thesis Supervisor

Accepted by: ....
....
Lallit Anand
Chairman, Department Committee on Graduate Students

This page is intentionally left blank.

Visual-based Methods in Compliant Mechanism Optimization

by

Richard W. Timm

ABSTRACT

The purpose of this research is to generate visual-based methods for optimizing compliant mechanisms (CMs). Visual-based optimization methods use graphical representations (3-D plots) of CM performance to convey design information. They have many advantages over traditional optimization methods, such as enabling judgment-based design tradeoffs and ensuring robustness of optimized solutions. This research fulfilled the primary aims of determining (1) how to best convey decision-driving design information, and (2) how to interpret and analyze the results of a visual-based optimization method. Other useful tools resulting from this work are (3) a nondimensional model of a CM (a compliant four-bar mechanism) that may be used to maximize the information density of optimization plots, and (4) a new model of a compliant beam that establishes a link between beam stiffness and instant center location. This work presents designers with an optimization tool that may either be used to augment or replace current optimization methods.

This page is intentionally left blank.

BIOGRAPHICAL NOTE

Richard Timm was born on December 14th, 1981, in Minneapolis, MN. He graduated from Cornell University in June 2004 with a B.S. in Mechanical Engineering. During a period of study abroad from February to June 2002, he attended the Technische Universität Dresden in Germany. Richard began work as a graduate student at MIT in the Precision Compliant Systems Laboratory in September 2004 and finished in December 2005 after 3 semesters of work. This thesis is the culmination of the work he did at MIT.

This page is intentionally left blank.

ACKNOWLEDGEMENTS

This page is intentionally left blank.

TABLE OF CONTENTS

LIST OF FIGURES

LIST OF TABLES

This page is intentionally left blank.

CHAPTER 1

1 INTRODUCTION

1.1 Purpose and essence of this research

The purpose of this research is to create visual-based methods for optimizing and analyzing compliant mechanisms (CMs). It is hypothesized that visual-based methods may be used to more efficiently and effectively present relevant decision-driving information. This is in contrast to the largely quantitative, equation-based, and numerical methods that dominate the conventional CM design process. Although quantitative methods make it easy to perform automated simulation and analysis of CMs, they are not well-suited to help a designer conceptualize and understand CMs. Simply put, designers rarely visualize equations and numbers when they design; they tend to visualize shapes and/or shape changes that can be related to, and described by, equations.

The new visual-based methods are focused around the use of 3-D plots to:

(1) Optimize mechanisms described by relatively few, e.g. on the order of six design variables

(2) Explore the local design space of mechanisms to gain understanding of the link between design parameters and performance

(3) Evaluate the results of a compliant mechanism (CM) optimization procedure

The integration of these methods within the CM design process makes the process more robust. Robust in this context refers to improving the process by enabling (1) a designer to become aware of potential problems manifested in an optimized design and (2) a designer to change the design to avoid such problems. The improvement is realized due to the fact that the visually presented information may more easily be interpreted, and therefore better utilized, in the course of making design decisions. Figure 1.1 shows the general CM design process and the stages in which the proposed methods would be useful.
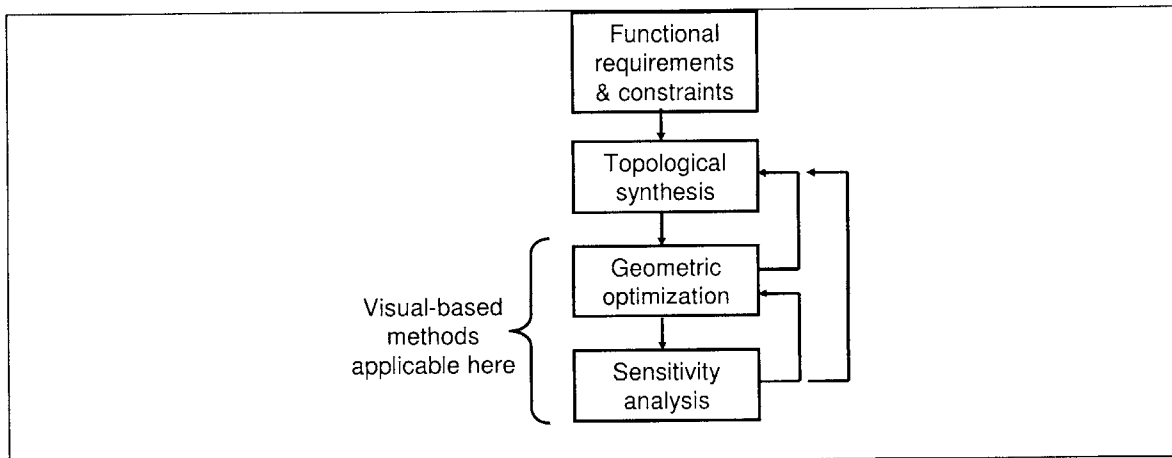
Figure 1.1: Conventional CM design process

Another benefit of using visual-based methods is that the methods reduce the amount of data that is necessary to convey relevant and actionable design information. That is, the data is provided in a format wherein the pertinent design issues, rules, and sensitivities may be readily extracted by the user. For example, conventional CM design processes often rely upon stiffness matrix

analysis which is not readily interpreted in a sense that is meaningful to understanding how a design works or can be improved. A designer is hard pressed to look at a stiffness matrix and identify the important nominal design parameter-performance relationships and/or the sensitivity of these relationships. This work aims to transform the conventional types of information in into forms that are better suited for rapid "human side" processing. Human side processing in this context is defined as pattern/trend recognition, data evaluation, and decision making. It is the decision making component of human side processing that is the most fundamental aspect of the design process. The purpose of all design tools and information should be to aid the designer in making better and more informed decisions. Three dimensional performance plots are used to exploit human's innate pattern recognition abilities to comprehend large amounts of data, and thus present the information needed to make decisions.

An example is used here to better explain the preceding. A mechanism and one of its associated performance plots is shown in Figure 1.2. Many design-relevant issues become clear upon inspection of such a performance plot. For example, Figure 1.2 may be used to ascertain performance minima, maxima, the bounds of manufacturing tolerances, and regions of high/low sensitivity. The use of similar plots can provide designers with other types of relevant design information in a more clear and concise manner when compared to conventional means.
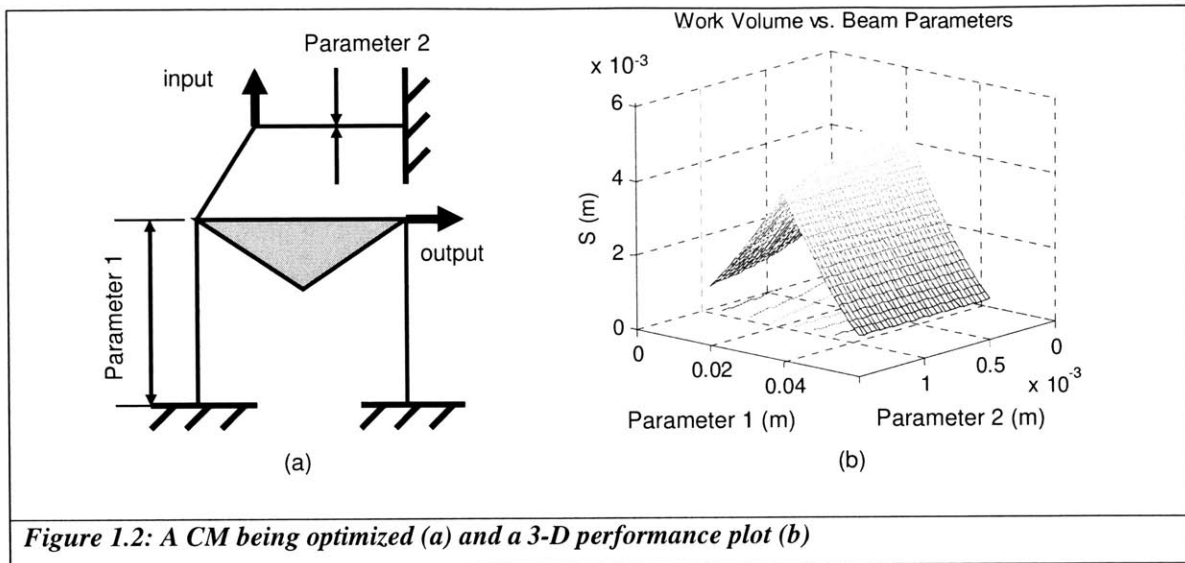
Figure 1.2: A CM being optimized (a) and a 3-D performance plot (b)

1.1.1 Important considerations

When faced with the possibility of improving the display of information via plots, one should address the maximum amount of information that may be displayed via plots. The information density of a plot may be improved if the axes of a performance plot are nondimensionalized to capture the effect of more variables. A model of a nondimensionalized compliant four-bar mechanism is presented in this thesis as a building block for other mechanisms. The nondimensional model can be used to:

(1) Design compliant four-bar mechanisms with respect to several important performance metrics.

(2) Demonstrate the general approach for obtaining relevant nondimensional parameters, which may be applied to the nondimensionalization of other CMs.

A primary hypothesis of this work is that the proposed visual-based approach gives designers the necessary information that is easily interpreted so that they may evaluate and understand

conceptual designs with respect to their performance. Visual assessment and interpretation represent a fundamental difference in approach that has not been previously proposed in theory or used in practice.

The proposed optimization method differs from conventional optimization methods in that it does not necessarily rely on the maximization of some objective function. Rather, it relies on the designer's own observation and judgment to adjust parameters to meet design requirements. This has distinct advantages and disadvantages. The advantages are that the designer is given the information and ability to make design tradeoff decisions. This can ultimately lead to a better-performing design and might be useful when the design requirements of a mechanism do not prescribe one of the performance metrics to be fully maximized or minimized. A specific application is the design of a precision motion stage where only a few performance metrics may be of interest, e.g. transmission ratio and nominal stiffness, and specific values of these metrics are sought.

As a further benefit, optimization using visual-based methods does not require the formulation of an objective function. Especially when multiple objectives are involved, formalization of the objective function requires an in-depth understanding and detailed estimation of how different performance metrics should be weighted in terms of final contribution to the objective function. A step is removed from the optimization process by not requiring an objective function.

A disadvantage of the proposed methods may present itself when a performance metric must be maximized or minimized. This type of application occurs when the success of the device is directly correlated to the degree to which its performance is optimized. Such a case may occur for instance in optimizing a MEMS transmission to have a high transmission ratio. If cost is

21

directly related to the size of the footprint of the device, and the footprint depends upon the transmission ratio, a 1% decrease in footprint may translate to 1% reduction in production costs. The error introduced by parameter selection using visual-based methods may be unacceptable in such cases.

1.1.2 Intellectual contribution

Specific items learned through this research include:

1.   Determination of the approach to find the nondimensional parameters required to optimize a compliant four-bar mechanism. Nondimensionalization of the parameters in performance equations enables a designer to normalize parameters, offering insight into the scaling relationships between mechanism parameters and performance.

2.   Determination of how to interpret, analyze, and use the data contained in performance versus mechanism parameter plots. Performance plots contain information that can offer insights into mechanism function, which is key to their understanding. Examples include sensitivities, minima, maxima, and the meaning of "features" in performance plots. Features are visibly conspicuous shapes on performance plots that have meaning relevant to CM design. This is explained further in Section 1.3.2.

3.   Formulation of a new compliant beam model more relevant to CM design and analysis. Compliant beams change in stiffness as their end conditions change. The model presented in this thesis offers insight into how stiffness changes with respect to the instant centers around which the ends of compliant beams rotate. This is vital in that it enables nondimensional analysis and is more broadly applicable to compliant four-bar design.

1.2 Background

1.2.1 Compliant mechanism design challenges

Compliant mechanisms are well-suited for many motion generating/guiding applications. Fully compliant mechanism have zero backlash and a direct correlation between force and displacement, which makes them ideal for applications in precision engineering, such as creating precision motion stages [1]. In addition, their potential to be manufactured monolithically greatly simplifies their manufacture and assembly and reduces cost in consumer applications such as shampoo bottle caps, backpack buckle clips, etc. Unfortunately, CM design is not trivial. The designer must simultaneously solve kinematic and elasto-mechanic requirements of the CM. When these problems are coupled, they become more difficult to solve, and these difficulties have in-part hindered the widespread use of CMs.

The fundamental issue that has led to this trouble is the nature of the information which is used to solve the coupled kinematic/elasto-mechanic equations. The conventional approach to CM design uses stiffness matrix analysis or similar quantitative methods. In general, these approaches must be quantitative in order to capture the complex behavior of elastic mechanisms. The draw back is that the CM design/behavior logic which is captured by these methods is generally embodied in a large number of numbers/terms/elements. In even the simplest of CMs, there are far too many terms for a designer to interpret and then understand or "see" how they relate to each other and affect the design. In the absence of the ability to "see" how the equations describe a CM's design behavior, it is difficult to use the information in raw form to make decisions that are fed back into the design loop.

One of the goals of this research is to take the data that would normally be contained in matrix form and convert it into a form that is more easily understood by designers. Anything that can

23

increase the ease of designing CMs may encourage their more widespread use. An example scenario of this is as follows: a designer has a specific application where the use of CMs has identified as a good design solution. However, the designer has no knowledge of CM design or understanding of how they work. The designer proceeds to read about topological synthesis and optimization (described in 1.5.1), which is a powerful and useful method to generate CMs. After using standard design software to generate and optimize a CM concept, the concept is brought to a design review where it is questioned. The designer has no understanding of why the design was made that way and no understanding of why one part of the mechanism has the shape it was given. The lack of this knowledge harms the case for using the CM, because so many unknown quantities would remain. In industries where the lack of this knowledge is unacceptable, e.g. medical devices, another technology would likely be selected.

There are several optimization methods that can be applied to CMs. The following subsections describe the most common methods.

1.2.2 Nonlinear optimization

In many cases, the important performance metrics for compliant mechanisms vary nonlinearly with respect to the geometric parameters that describe them. As a result, CM design optimization requires nonlinear optimization techniques. The conventional optimization occurs in three steps [2]:

1. System definition – determination of the physical bounds of the design space, the input and output definition (force, displacement, work piece model)

2. Formulation of objective function – a numeric measure of system performance. In CMs, such objective functions may include the metrics listed in Section 1.4.

3. Design space search using the appropriate algorithm, such as nonlinear programming [2] or the Method of Moving Asymptotes [3], which is commonly used for optimizing CMs.

A general optimization problem can be stated by the following equations and inequalities:

Optimize $F = f(x)$ $\qquad$ (1.1)

Subject to:

$h(x) = 0$ $\qquad$ (1.2)

$g(x) \leq 0$ $\qquad$ (1.3)

Where F is the objective function to be solved, x contains the variables (dimensions) of the design space, and h and g are the constraints imposed upon the design space. An example of what the output of an optimization algorithm involving five parameters might look like Equation 1.4. It is essentially a vector that contains the optimized values of the mechanism parameters.

$$PARAMETERS = \begin{bmatrix} 1.2 \\ 0.04 \\ 0.7 \\ 0.03 \\ 0.125 \end{bmatrix} \qquad (1.4)$$

Optimization procedures can run blindly and unpredictably into poor solutions, which makes it critical to analyze the output of any optimization procedure. The fundamental issue here is that an optimization algorithm is only as good as the objective function and imposed constraints. These constraints and the objective function capture the raw mechanism performance, but to

25

ensure robust solutions, the optimization algorithm would have to capture some measure of the robustness of the performance as it relates to unknown factors in the system, e.g. manufacturing tolerances, actuator misalignment, etc. Visual-based methods provide information about the design space surrounding the optimized solution and give the designer the tools and information needed to determine whether a particular optimization solution is robust to such variations. Sensitivity analysis is a partial solution to some of these issues, and it is described in the following section.

1.2.3 Sensitivity analysis

Sensitivity analysis is the process of determining how design parameters affect performance for a given point in the design space. Knowing the sensitivity values for a particular mechanism enables a designer to decide for instance acceptable fabrication tolerances. The type of sensitivity that is useful for comparison with manufacturing tolerances is called the dimensional sensitivity [4]. The equation that defines dimensional sensitivity is given in Equation 1.5.

$$\text{Dimensional sensitivity} = \frac{Z(X + \gamma) - Z(X)}{Z} \tag{1.5}$$

The output of a sensitivity analysis may be similar to that of an optimization routine – a vector containing sensitivity values for each mechanism parameter. An example of what this might look like is given in Equation 1.6.

$$SENSITIVITY = \begin{bmatrix} 0.01 \\ 1.00 \\ 0.00 \\ 0.32 \\ 0.04 \end{bmatrix} \tag{1.6}$$

A drawback of displaying information in this manner is that it does not take into account the surrounding design space. As is discussed in Section 2.3, sensitivity has the ability to change abruptly within the limits of some manufacturing tolerances. This is hazardous to the operation of the mechanism and must be addressed by modifying the design process. Visual-based methods address this issue by displaying the local design space to the user. Not only is sensitivity shown, but abrupt changes in the sensitivity as well.

1.3 Visual-based optimization methods

Visual based optimization of CMs is carried out by using a series of plots that compare performance metrics of interest to parameters that describe the mechanism. Each performance plot is capable of displaying performance on three axes: one axis for performance and two axes for parameters. The number of dimensions that may be perceived at once is three, limiting the amount of information that can be displayed at once. For systems described by more than two parameters, performance plots must be generated successively for each set of parameters. Following the optimization of the mechanism with respect to each parameter in succession, the performance must be validated. If validation shows an unsuccessful optimization has occurred, the process must be iterated. The process of optimization and validation of a mechanism with N parameters is summarized in Figure 1.3.

Figure 1.3: Visual-based optimization and optimization-validation process
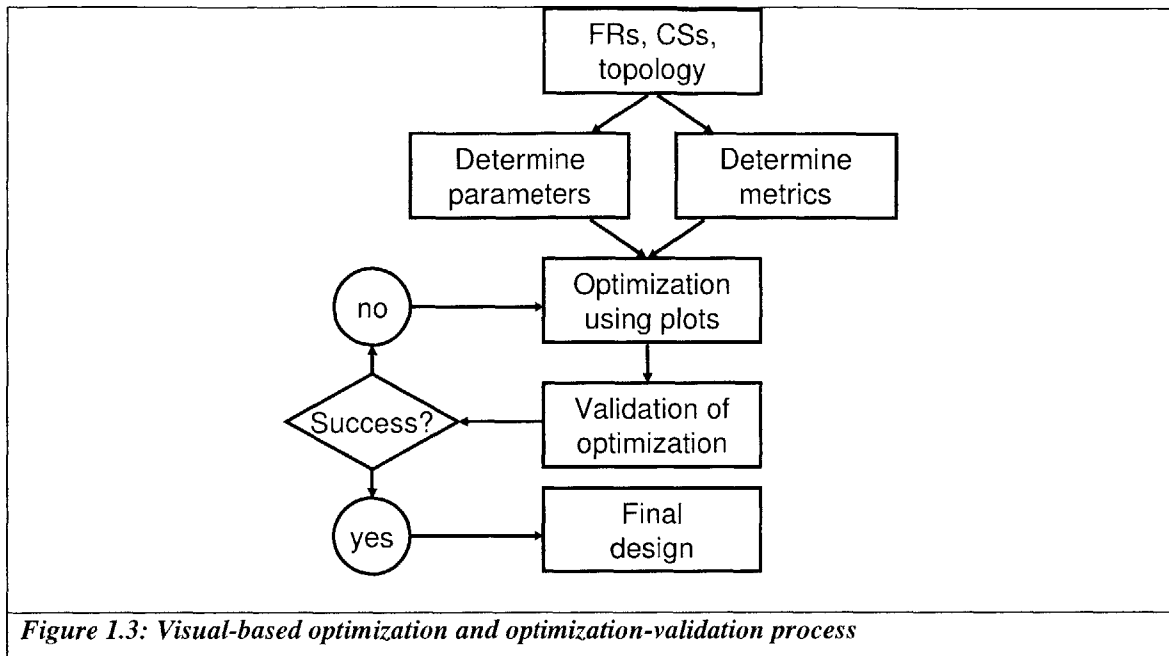
There are two steps that are not captured by Figure 1.3. The first is the selection of the appropriate performance metrics, which are usually based upon the system requirements. The second step is choosing the parameters that describe the system. Often times design intent is incorporated into the system model to help select parameters. Two types of parameters may be used: dimensional or nondimensional. Dimensional parameters are useful for optimizing a mechanism to meet specific requirements. Nondimensional parameters are useful for understanding specifically how performance scales with parameters, as well as how the normalization of parameter groups reduces the overall number of parameters that must be considered.

1.3.1 Compliant mechanism optimization, sensitivity analysis, and design tradeoffs

In this research, the optimization method differs from those discussed in 1.2.2. The proposed method produces graphs that plot CM performance vs. mechanism parameters in a manner that is well-suited to CM design. These graphs may show the designer many items of importance, for example:

28

(1) The sensitivities, i.e. gradients, of certain performance metrics with respect to design parameters. Figure 1.4 is a plot of two important mechanism parameters (stiffness and range of motion) as they change with one particular mechanism dimension. Sensitivity data is useful in point (2).

(2) Design tradeoff decisions use sensitivity data to compare various performance metrics. Often times, performance metrics are competing factors, meaning that increasing one often means decreasing the other. A prime example is that as the stiffness of a mechanism increases, its elastic range decreases. Figure 1.4 gives the designer the information necessary to make a design tradeoff decision between these two factors. An example of where this is of prime concern is in a vibration attenuation device, where a large range of motion is desired while keeping an adequate stiffness [5].

29
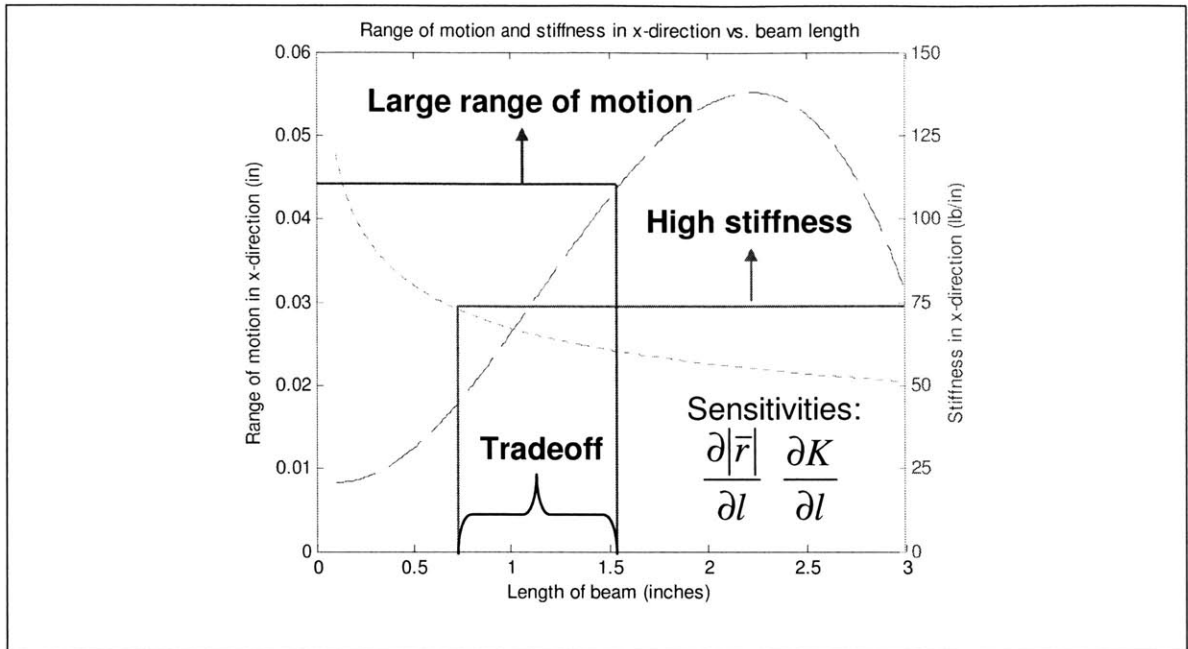
Figure 1.4: A plot showing the minima, maxima, and sensitivities of stiffness and range of motion versus a particular CM parameter

(3) The minima and maxima in performance plots. Often times, an optimization procedure seeks to minimize or maximize a particular performance value. Such minima and maxima in performance are instantly apparent when the data is displayed using a plot.

(4) Features that are indicators of fundamental change in the CM's internal workings. Features are discussed further in Section 1.3.2 and illustrated by Figure 1.6. Features are "sudden changes" in the sensitivity in a plot. They can prove dangerous for a traditional optimization algorithm if it "picks" a point in the design space near a feature, at which the performance may abruptly veer out of specifications. Visual-based methods present information in a way that makes features apparent to designers, so they are aware of them when choosing the CM's point of operation in the design space.

In addition, this work describes polynomial equations that can be fit to multi-dimensional performance data. Polynomial equations are more easily understood than matrix equations. The preceding approach is proposed in order to provide designers a more accurate means of quantitative assessment that compliments the qualitative and quasi-quantitative information that may be perceived from the plots. The equations also provide a "handshake," which enables the design info to be shared with computer-based tools. The combination of visual qualitative and quantitative data forms the basis for a powerful pair of design tools.

1.3.2 Features in compliant mechanism performance plots

Features, i.e. locations of high slope change, within the surface of CM performance plots may be indicators of changes in the CM's internal workings as shown in Figure 1.6. The term "internal workings" means information such as the region of maximum stress, as well as the transmission ratio. Figure 1.5 shows a multi-axis compliant mechanism. Figure 1.6 contains performance plots of this mechanism. The plots show discontinuities in range of motion versus a specific beam element dimension, which indicates a change of location of the maximum stress. The location of maximum stress refers to the specific beam element in the CM that experiences the highest stress. In addition, the transmission ratio for a CM may go to zero or change signs with a change in CM dimensions.

Figure 1.5: A compliant mechanism (a), the symmetric change of the thickness of beam B (b), and the symmetric change of the length of beam A (c).

Figure 1.6: Plots showing change in location of maximum stress (a) and a change in the transmission ratio (b) of the same CM as compared to two CM dimensions
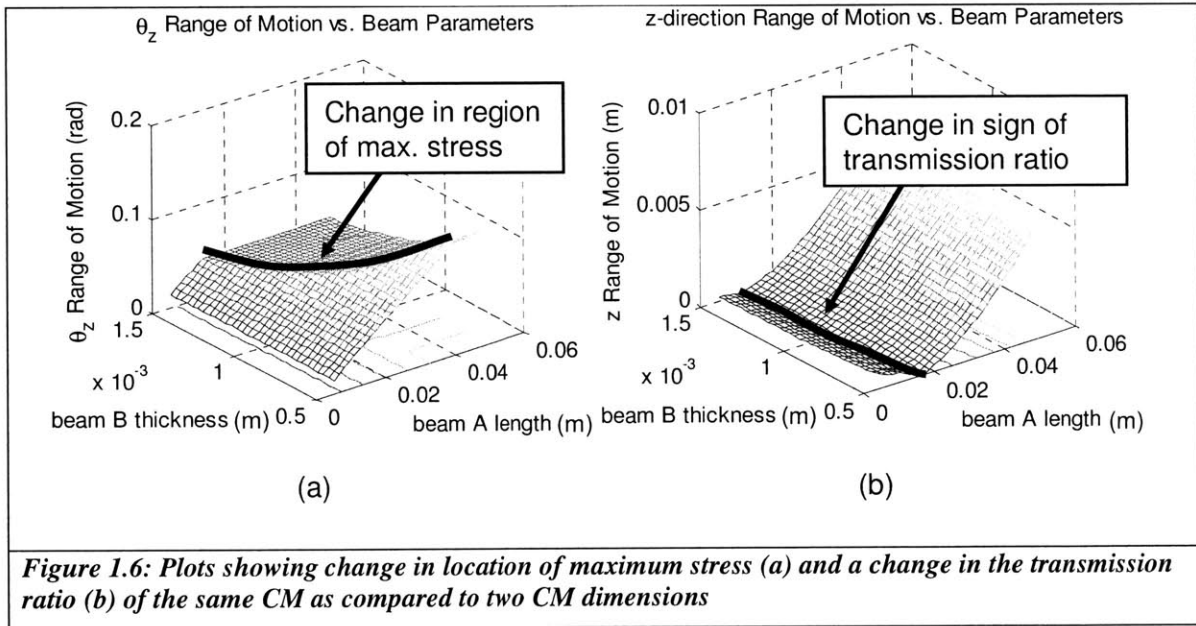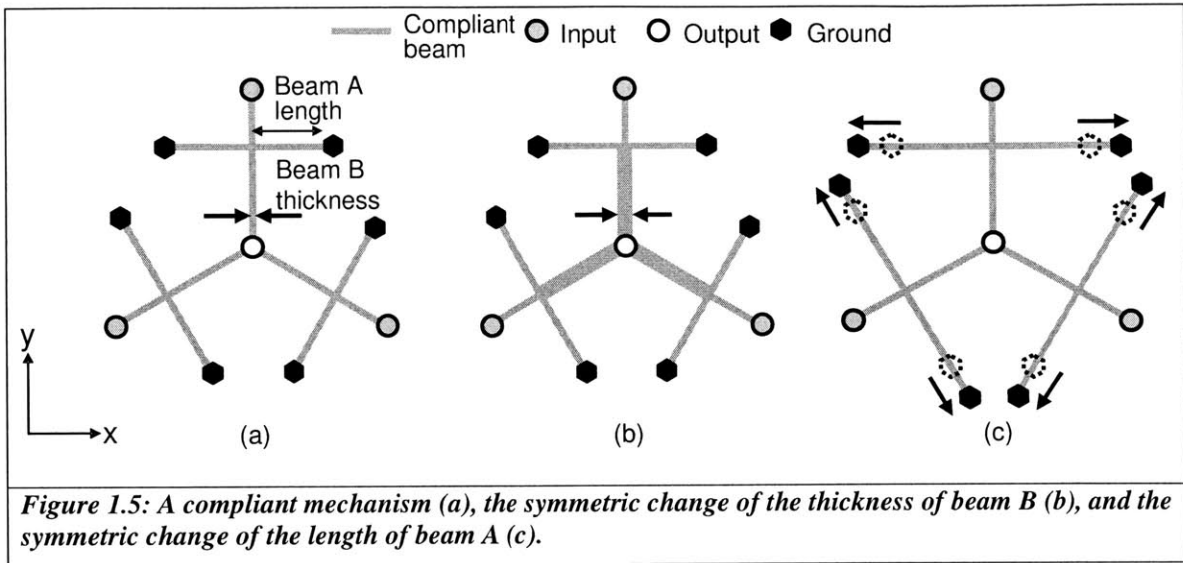
1.4 Important performance metrics in CM design

Compliant mechanisms are often designed to satisfy functional requirements such as:

Work volume, S

Work volume in the context of this thesis always refers to the mechanism-limited work volume. At the limits of the work volume the mechanism fails due to plastic yielding. The work volume is then defined as the range of motion of the mechanism's output as actuated at the input before it yields. One of the key design challenges in CM design is ensuring that they can move over a large enough range to perform the necessary function(s).

Nominal input stiffness, $K|_{input}$

Nominal stiffness is the measured stiffness at the input of a mechanism. The nominal stiffness of the mechanism must be known when incorporating actuators into the system if one wishes to maximize performance of the actuator.

Transmission ratio, Tr

The transmission ratio is the ratio of the output, x_2, motion of a CM divided by the input motion, x_1. It can be found from equation 1.7.

$$Tr \equiv x_2 / x_1 \tag{1.7}$$

It is necessary to know the transmission ratio in order to know if the actuator input must be amplified or attenuated.

Efficiency, η

Compliant mechanisms do not transfer all of the input energy to the output. The energy efficiency is given below:

$$\eta \equiv \frac{E_{out}}{E_{in}} = \frac{F_2 x_2}{F_1 x_1} \tag{1.8}$$

It is necessary to know the efficiency if the CM is used to transfer energy or force. Efficiency is a measure of how well the input and output are kinematically linked. The efficiency is a function of the mechanism stiffness and the nature of the output.

1.5 Conventional modeling and design approaches

1.5.1 Topological synthesis and optimization

Topological synthesis is a method of automatically generating CM concepts based on a set of performance requirements. At the heart of topological synthesis of CMs is a computer optimization algorithm that automatically generates and quantitatively compares performance of different CM concept topologies and then selects the best one [6-11]. In a subsequent performance optimization process, the dimensions of the selected concept are modified to produce the best-performing solution. Topological synthesis methods are usually able to generate CM concepts when a design scenario is properly set up by the designer. The result of a topological synthesis procedure is a CM concept and some quantitative measure of its performance (the objective function).

Although topological synthesis and related optimization methods are ways of creating and optimizing feasible compliant mechanism concepts, the designer is decoupled from the design decision loop and therefore may not understand the nature of the design. As a result, the designer may not be able to ascertain how to change the design or integrate it into a system as he or she does not fully understand how it works. For this reason, it would also be difficult to incorporate visual-based optimization methods in a topological synthesis procedure; the designer would not

be aware of the design intent captured in the model. This lack of understanding would make it difficult to choose the correct and minimum number of parameters necessary to optimize the mechanism.

1.5.2 Traditional rigid mechanism synthesis and the pseudo-rigid body model

There are two methods that are used to design traditional rigid mechanisms: graphical (geometric) synthesis and analytic methods using vectors loops. The pseudo-rigid body model (PRBM) provides an effective means of analyzing the compliant analogs of traditional mechanisms [12]. Shooting methods, FEA, and other methods are then employed to optimize and compare CM concepts.

Visual-based optimization methods are compatible with traditional mechanism synthesis techniques, as the designer would have a good idea of what critical design intent is captured in the concept. Traditional mechanism synthesis and analysis tools, e.g. instant center analysis, provide the necessary design intent information to choose the proper parameters for CM optimization [17]. Thus, the minimum number of visual plots could be used to optimize a mechanism and understand its performance over the design space.

1.5.3 Constraint-based design

Constraint-based design is an approach that is based upon a set of mechanical design principles that have been developed for the design of precision machines [13-15]. Constraint-based design selectively combines constraints and degrees of freedom to create designs with the desired kinematics. The resulting degrees-of-freedom correlate to desired motion. When this method is applied to CM synthesis, the constituent compliant elements are modular elements that are stiff in some directions and compliant in others.

Visual-based methods are ideally suited to optimize compliant mechanism concepts that are generated using constraint-based design principles. The knowledge of these principles aids in selecting the proper parameters for optimization, and the data generated using visual-based methods symbiotically fosters further intuition of the how CM performance relates to design parameters. In practice, the layout of constraints can be included as design parameters. For example, the angle of a particular compliant element/constraint could be chosen as a parameter to vary. Changing the angle of a constraint could have the potential to affect all of the important performance metrics, as it may directly manipulate the kinematics of the mechanism.

1.6 Hypotheses

Although the primary hypothesis of this thesis has been discussed in moderate detail, it is important to understand several other hypotheses that stem from the conception of the primary hypothesis. The set of hypotheses addressed via this thesis relate to:

1. Visual-based optimization and post-optimization analysis methods

The methods proposed in this thesis can be used in an optimization process that does not rely on a single objective function (i.e. quantitative metric of system performance). The lack of an objective function allows for a more flexible optimization process in that the designer has the power and necessary information to make design tradeoffs between different performance metrics. This flexibility is useful when designing mechanisms where requirements are not difficult to meet, or where the absolute maximum of any performance metric is not crucial to the success of the mechanism. Specific examples exist in precision engineering in designing motion stages where the requirements and constraints for stiffness, range of motion, and transmission ratio do not exclude a large portion of the design space.

2. Amount of information necessary to optimize mechanisms using visual-based methods

The information necessary to optimize a mechanism described by N parameters for P performance metrics is equal to or less than $P*N$ 2-D plots, which can be condensed into $P*N/2$ 3-D plots. It is important to reduce the number of plots examined to reduce the overall time required to optimize a mechanism using visual-based methods. This is proved via a case study and the logical discussion following.

3. Nondimensional analysis

Nondimensional analysis can reduce the number of variables necessary to perform optimization of a CM with respect to performance metrics of interest. This is important because nondimensionalization allows abstraction from specific dimensional values, which lends insight into how the scaling of mechanism parameters impacts mechanism performance.

4. Visual-based data analysis vs. other

Visual representations are able to efficiently convey important design-relevant information to designers. Other methods of conveying the same information require far more mental effort as the reader will find through subjective evaluation of different methods. The "other" methods of conveying design information include using numbers, vectors, equations, and matrices. Visual-based methods derive their efficiency by exploiting humans' innate ability to process visual data in the form of shapes.

The preceding hypotheses will be examined in Chapter 5.

1.7 Thesis organization

Chapter 2 provides a qualitative discussion of the link between the compliant mechanism design process and user perception of design information. Design information in this context means performance data (e.g. transmission ratio, efficiency, etc.) as it relates to the parameters that describe mechanism geometry. This performance data is contained within the matrices used to model CMs. The transfer of that data into a comprehensible form is the key challenge that is addressed in Chapter 2. Chapter 3 contains the technical information about how performance data is extracted from matrix form and converted into a visual format. A nondimensional model of a compliant four-bar mechanism is presented in Chapter 4. Also, a new model of a compliant beam is derived that is an accurate model of beam bending in compliant mechanisms. The nondimensional parameters that are produced by the new model are used to present performance information in a denser format than using dimensional parameters. Chapter 5 contains a case study in compliant mechanism optimization using visual-based methods. The case study is used to prove the research hypotheses of this thesis. Concluding remarks and a recap of the research contributions and proposals for continued work are provided in Chapter 6.

CHAPTER 2

2 ASSESSMENT OF THE LINK BETWEEN THE COMPLIANT MECHANISM DESIGN PROCESS AND DESIGNER PERCEPTION OF DESIGN INFORMATION

The purpose of this chapter is to elucidate the reasons why visual-based methods were proposed as a useful tool in the CM design process. This chapter contains a qualitative discussion of visual-based methods (VBMs) and how they contrast with the alternatives. Emphasis is placed upon the reasons why VBMs are beneficial in conveying important design information. The motivation for a new method is the need to increase the ease and efficiency with which design information is perceived and interpreted by the designer. To accomplish this, the relevant performance metrics must be compatible with both the means of computer expression and the way designers think. The first step in assessing whether VBMs are indeed more efficient is to determine what information is required to (1) optimize a CM and (2) process the results. This

information provides a framework for determining how the relevant information could and should be displayed to designers. Figure 2.1 shows schematically how information flows in the optimization procedure and highlights where VBMs are applicable.

Figure 2.1: Information flow in the optimization process
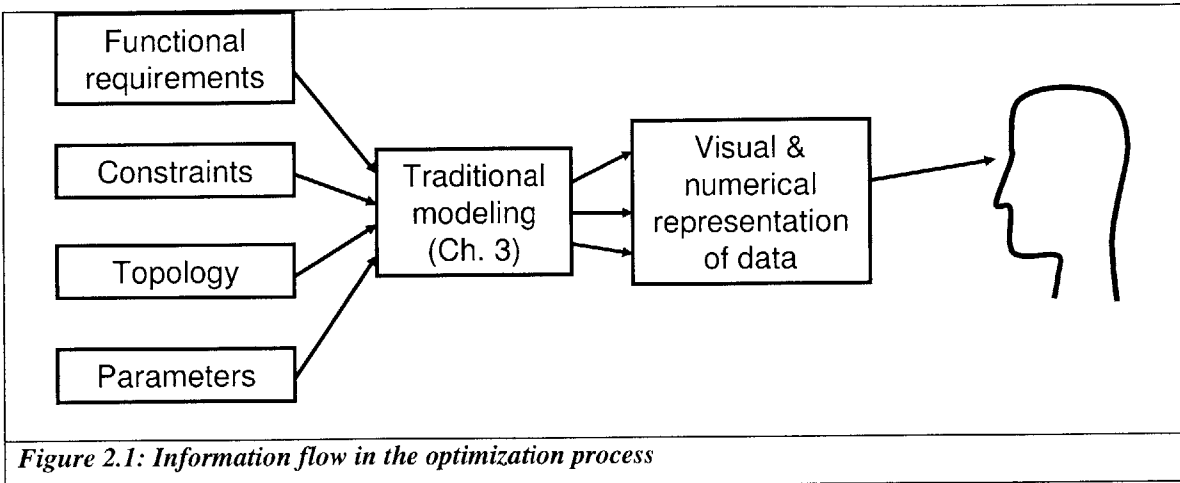
2.1 Information required to perform CM optimization

Before proceeding, a brief overview of design vernacular is provided.

2.1.1 Mechanism functional requirements (FRs)

The functional requirements of a CM are combined to form a list of what specifically the mechanism must do within a specified tolerance [16]. Metrics are attached to these requirements to provide an objective measure of how well a given mechanism fulfills them. At the same time, there is also acceptable variation attached to such requirements — it would be unrealistic in most scenarios to attempt to design a system to exactly meet every requirement. A list of some of the most important FRs for compliant mechanisms is given in section 1.4.

2.1.2 Design constraints

Design constraints are the factors that define the limits of the design space. In CM design, these limitations may include the size of the mechanism, the materials used, the fabrication processes

40

used, etc. Design constraints are different from functional requirements in that they are not explicit measure of mechanism function, i.e. what the mechanism is designed to do or perform. Design constraints are binary, meaning they are either met or not, whereas FRs have a window of tolerance.

2.1.3 Mechanism topology

The rigid mechanism analogy of compliant mechanism topology is called the mechanism "type" [17]. It is a description of how the elements of the mechanism are connected to each other. In the context of compliant mechanisms consisting of flexible beams and rigid elements, the topology would describe how the various beams, rigid links, inputs, outputs, and grounds are connected to each other. Topology formulation can be decoupled from geometric optimization to simplify the design process. The decision to decouple these steps is a tradeoff: it eliminates part of the design space by solving for some of the system parameters first (the ones describing topology) and subsequently optimizes the remaining (geometric) parameters. Some optimization methods do not decouple these steps and use a genetic algorithm to capture the mechanism's topology and geometric parameters simultaneously [18-20]. When topology formulation and geometric optimization are not decoupled, the design space remains accessible throughout the process.

2.1.4 Mechanism design parameters and design intent

The mechanism design parameters (DPs) are the set of independent values that are required to fully determine the dimensions of a mechanism, i.e. beam lengths, thicknesses, rigid body sizes, etc. The parameters may be defined in any way the designer wishes so long as they fully describe the mechanism's shape. The important issues are that DPs be defined in such a way that:

(1) As the parameters vary, the intent of the design is preserved

(2) The link between parameters and mechanism dimensions is readily apparent

Point 1 is especially important because losing design intent could completely change the function of the mechanism or impair performance. Point 2 is important because it is good design practice to maintain clear links between parameters and dimensions when possible.

To put the idea of design intent in more concrete terms, Figure 2.2 shows two ways of defining the parameter of the same mechanism such that the first preserves design intent and the second does not. The purpose of this mechanism is to "deamplify" the input of a displacement actuator given an output stiffness. The constraints on the design are that the actuation occurs in the positive x-direction and the output moves in the negative y-direction. Instant center analysis of Figure 2.2 (b) shows that certain combinations of parameters violate the design intent regarding the output motion, i.e. the motion would not always be in the negative y-direction. Thus, the design intent is not preserved. Instant center analysis is a fast method of determining whether design intent is preserved in defining mechanism parameters.

Figure 2.2: Examples of different ways of defining the parameters of the same mechanism. The design intent is preserved in (a) and lost in (b).
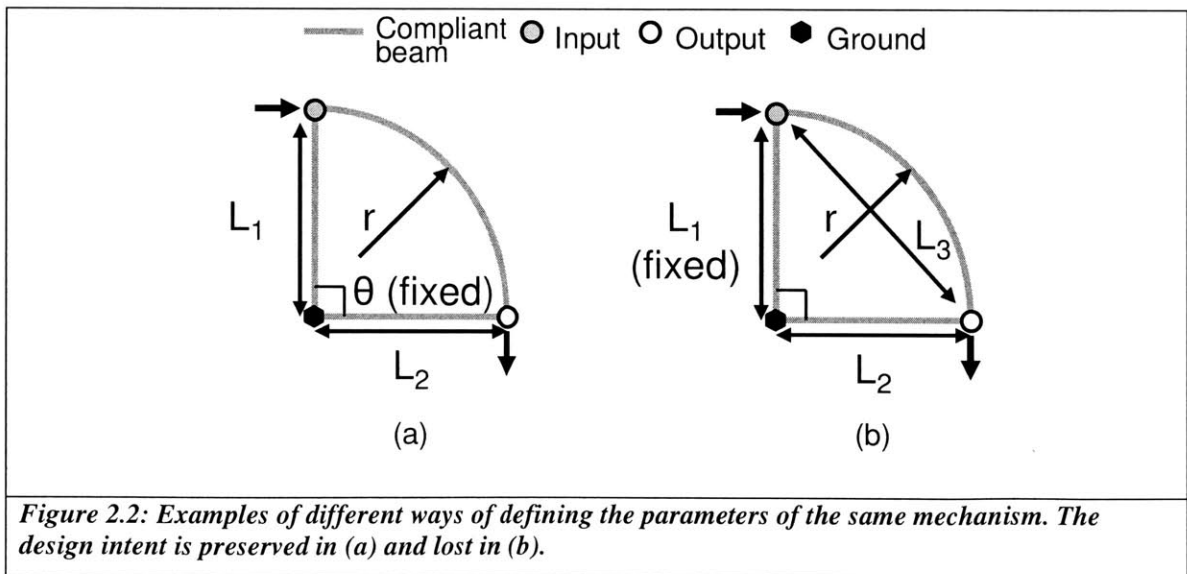
2.2 Conveying design information

The most general form of performance information for a mechanism is contained within the models used to describe it. In this thesis, the modeling method of choice is the stiffness matrix. Questions arise: How can the information contained within the stiffness matrix be distilled into a form that a designer can use to make decisions? What attributes should the new information have? There are several methods of conveying this information, which are discussed below.

2.2.1 Numbers and magnitudes

Numbers must ultimately be used to directly compare functional requirements with optimization results and sensitivity values. Numbers are useful for understanding limited amounts of data. All objective information is ultimately distilled into numeric form at some level. However, the brain becomes "overloaded" if too many numbers are observed at once. As stated previously, the output of an optimization or sensitivity analysis may be a vector containing numbers. However, displaying large amounts of data needed to show the design space immediately surrounding an optimal solution is impractical and impairs comprehension. The reader is encouraged to confirm this by looking at the data in Equation 2.1 and identifying the line in x and y coordinates where the sharpest change in slope exists. This example also demonstrates the point that it is important to look at the right type of data, and that the information density must be maximized without sacrificing comprehensibility.

Table 2.1: Numeric data in matrix form										
		y								
		0.00	0.25	0.50	0.75	1.00	1.25	1.50	1.75	2.00
x	0.00	1.00	1.03	1.06	1.09	1.13	1.15	1.16	1.14	1.07
	0.25	1.00	1.03	1.06	1.09	1.12	1.15	1.16	1.14	1.06
	0.50	1.00	1.03	1.06	1.09	1.12	1.15	1.15	1.12	1.03
	0.75	1.00	1.03	1.05	1.09	1.12	1.14	1.13	1.09	0.98
	1.00	1.00	1.03	1.05	1.08	1.11	1.12	1.11	1.04	0.91
	1.25	1.00	1.03	1.05	1.08	1.10	1.10	1.07	0.98	0.82
	1.50	1.00	1.03	1.05	1.08	1.09	1.08	1.03	0.92	0.71
	1.75	1.00	1.03	1.05	1.07	1.08	1.06	0.98	0.83	0.58
	2.00	1.00	1.03	1.05	1.07	1.07	1.03	0.93	0.74	0.43

As might be obvious, finding the location of sharpest slope change requires some thought to accomplish. On the other hand, it is easy to look at any individual value and compare it to a performance metric of interest. The information captured in Table 2.1 is also contained within Equation 2.1 and Figure 2.3 for comparison.

2.2.2 Equations

Equations contain more information than mere numeric values – they contain relationships between variables, show how variables scale and can be used to find closed-form analytic solutions. However, to extract useful information requires manipulation of variables, possibly taking derivatives, etc. While equations have more flexibility and contain more information than numeric values alone, to use them in post-optimization analysis of optimization results is equally difficult. As an exercise, the reader is encouraged to look at Equation 2.1 and determine where the sharpest change in slope, e.g. as might be found between the maximum sensitivity of range to

beam width, occurs over the ranges $x = [0, 2]$ and $y = [0, 2]$. As will be found, it is difficult to extract values and meaningful information from visual inspection alone.

$$z = -\frac{1}{200}x^4y^2 - \frac{1}{100}x^3y^2 - \frac{1}{24}x^4 + \frac{1}{15}x^3 + \frac{1}{10}x + 1 \tag{2.1}$$

For contrast, Equation 2.1 is shown graphically in a 3-D plot in Figure 2.3. The reader will find that information on the sensitivity, plot minimum, and plot maximum are readily extracted through inspection of Figure 2.3.

2.2.3 Plots and visual-based representation of data
3-D plots of performance can be generated by converting data of the form in Equation 2.1 into a mesh or contour plot (or both). This essentially converts the data into a 3-D shape or surface and removes much of the abstraction from the analysis, as the mind is well-suited to perceive and evaluated 3-D shapes. 3-D plots lend a qualitative element that is of assistance in quantitative analysis. Looking at a 3-D plot of CM performance, the following questions can be answered immediately upon inspection:

1. Is the mechanism's performance in the right ballpark? (It should be if the mechanism's topology has been laid out well.)

2. Where is the performance insensitive to changes in parameter values?

3. Where is the performance highly sensitive to changes in parameter values?

4. Are there separate regions of high sensitivity and low sensitivity?

5. Where do minima/maxima occur?

6. For what parameter value ranges does the mechanism meet requirements?

The reader is encouraged to look at Figure 2.3 below and attempt to answer some of the questions posed above. Figure 2.3 contains the same information as Equation 2.1, except the data is shown in graphical form.
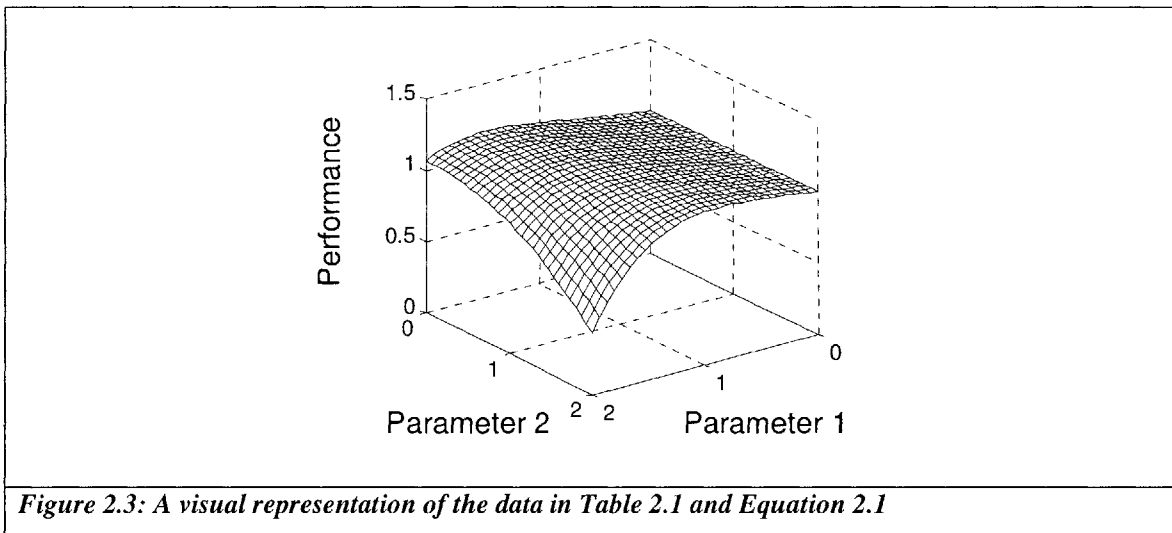
Figure 2.3: A visual representation of the data in Table 2.1 and Equation 2.1

The answers to the given questions are given in Figure 2.4.
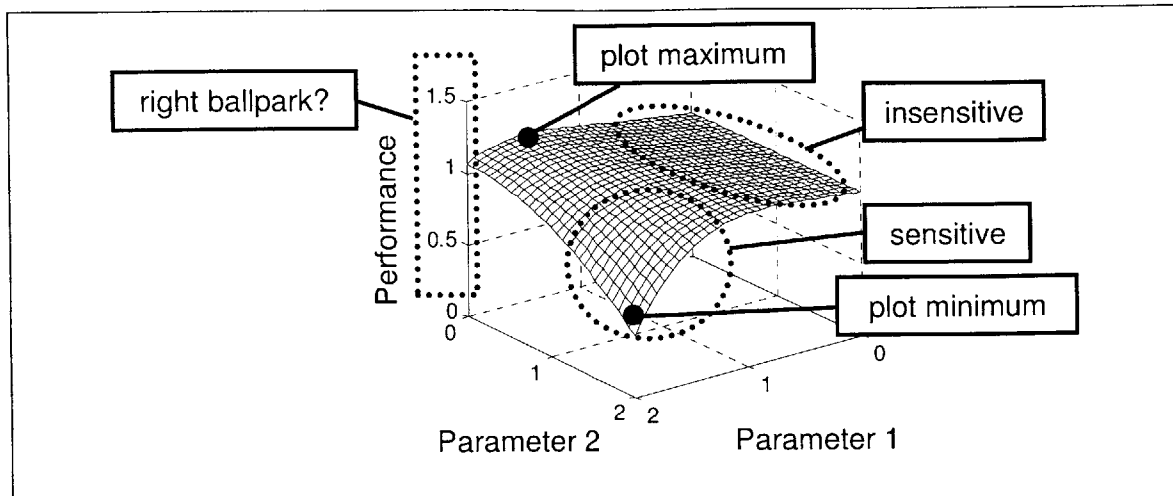
Figure 2.4: The answer key showing important design information
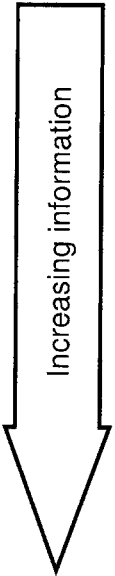
On the other hand, plots are not ideal for extracting exact numeric values. The process is limited by the resolution of the human eye working in conjunction with the plot axes. "Zooming in" on a plot and/or changing the mesh spacing may be the appropriate course of action if greater resolution is desired. Once the important initial questions have been answered (as given above), a designer must use numeric values for the final evaluation of performance.

2.2.4 CAD-type interface

A CAD-type interface is one that would actually show the optimized and dimensionally-accurate form of the mechanism. This type of visual display is only indirectly related to the above forms of data; it is not used to show performance per se, but rather to show the final shape of the mechanism and allow the designer to confirm that it (1) is a feasible design to manufacture and (2) satisfies volume constraints.

Table 2.2 provides a summary of the discussion in Section 2.2.

47

Table 2.2: Summary of different ways of displaying information and what they are useful for				
	Type of info. useful for optimization	Content of information	Utility of information	Disadvantages
Increasing information (↓)	Numbers	Nominal values, sensitivities	Straightforward comparison of CM performance to requirements	Limited amount of data can be perceived at once
	Vectors	Nominal values, sensitivities, trends	Straightforward comparison of CM performance to requirements	Limited amount of data can be perceived at once
	Equations	Nominal values, sensitivities, trends, scaling powers	Ability to see relationship between performance and parameters	Difficult to extract information from visual inspection
	Matrices	Containing all information of many equations simultaneously	Full description of mechanism design space	Overwhelming information that cannot all be comprehended at once
	Visual plots	Nominal values, sensitivities, trends, maxima, minima	Range of performance values, regions of high and low sensitivity, minima and maxima	Not good for determining exact values
	CAD type	Final shape of mechanism	Manufacturing feasibility, volume constraints	Not directly related to performance data

2.3 Features in performance plots

A feature can be described qualitatively as a sudden change in sensitivity of performance with respect to parameters (i.e. a "spike" in the second derivative of the performance). A feature exists when the slope changes within a given envelope (often determined by manufacturing tolerances) by more than a critical percentage. The critical percentage depends on the particular design

scenario, so the designer must investigate a suspected feature by "zooming" in on the plot by changing the mesh spacing and plot bounds.

Sensitivity analysis is performed only at the design point of interest. Features are important because they are usually not directly addressed by conventional optimization routines. Sudden changes in sensitivity in the local design space could pose a problem, as a conventional optimization procedure may choose an operating point next to or on a feature. This is not unlikely, as local minima/maxima in performance often lie on features. If manufacturing tolerances "straddle" a feature, the performance may suddenly deteriorate to unacceptable values within manufacturing tolerances. Therefore, the detection of such features becomes critical. Fortunately, VBMs are well suited to analyzing such a problem, as sudden changes in sensitivity often appear as qualitative features discernable to the eye. They are especially prevalent when looking at plots of the work volume of a mechanism, where they can occur as "folds" or "toughs." A fold appears as a crease along which two separate surfaces intersect. A trough appears as a valley where the work volume reaches zero for some combination of the mechanism parameters. The concept of folds and troughs is clarified in Figure 2.5.
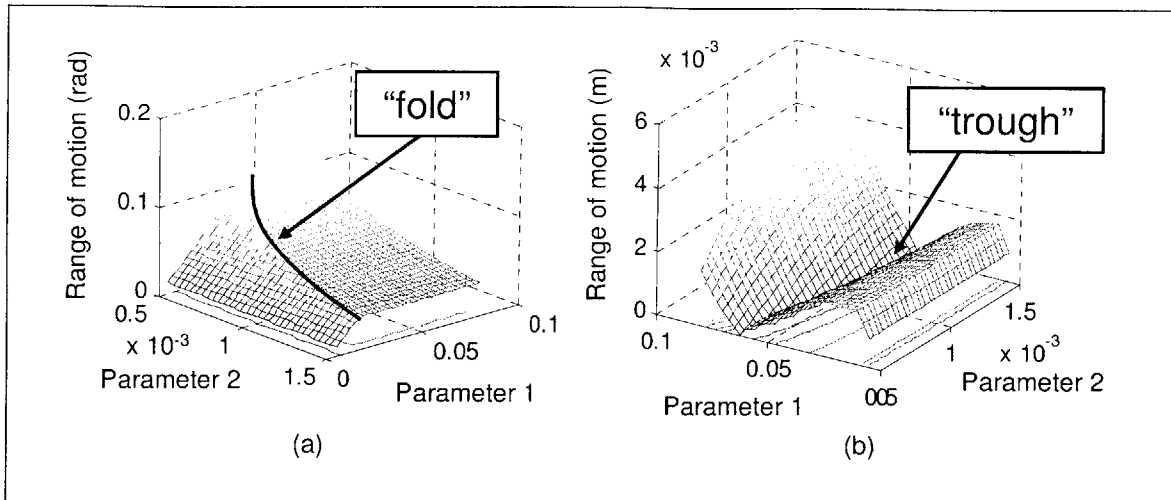
Figure 2.5: Folds and troughs in CM performance plots

The causes for folds and troughs in work volume plots are different. The cause of troughs is that the transmission ratio of the mechanism for a particular combination of parameters is zero. Work volume is defined as the range of motion of the output, and when the output ceases to move at all when the transmission ratio is zero, the work volume will also be zero. The cause for folds in work volume plots is more subtle. To examine the cause in depth, the method of finding work volume must be scrutinized.

2.3.1 Qualitative description of calculating the work volume of a CM

The first step in calculating work volume is to apply a proof force at the mechanism's input and record two pieces of information: the displacement of the output and the stress at every location in the mechanism. In a linear system, the stress and output displacement scale linearly as the magnitude of the proof force is changed. This knowledge allows the immediate calculation of work volume: the acceptable stress level in the mechanism is divided by the maximum stress observed under proof force loading. This non-dimensional factor is used to multiply the displacement under proof force loading to obtain the work volume of the mechanism.

2.3.2 The cause of folds in work volume plots

What could be the cause of a fold, or a sudden change in the shape of the work volume plot? The answer lies in the stresses in each part of the mechanism; as parameters are varied, the relative stress levels in different parts of the mechanism also change. When the maximum level of stress changes from one location in the mechanism to a different location, the work volume changes shape. Stresses in different components of the mechanism have different dependencies on the mechanism parameters being varied. The differences in shape are shown conceptually in Figure 2.6. For clarity, the work volume is calculated for each beam individually (denoted $S_i|_{output}$, where each i represents a different beam), and the results are combined to give the whole mechanism work volume. Note that it is now the minimum (or intersection) in work volume between the different mechanism components that must be used.
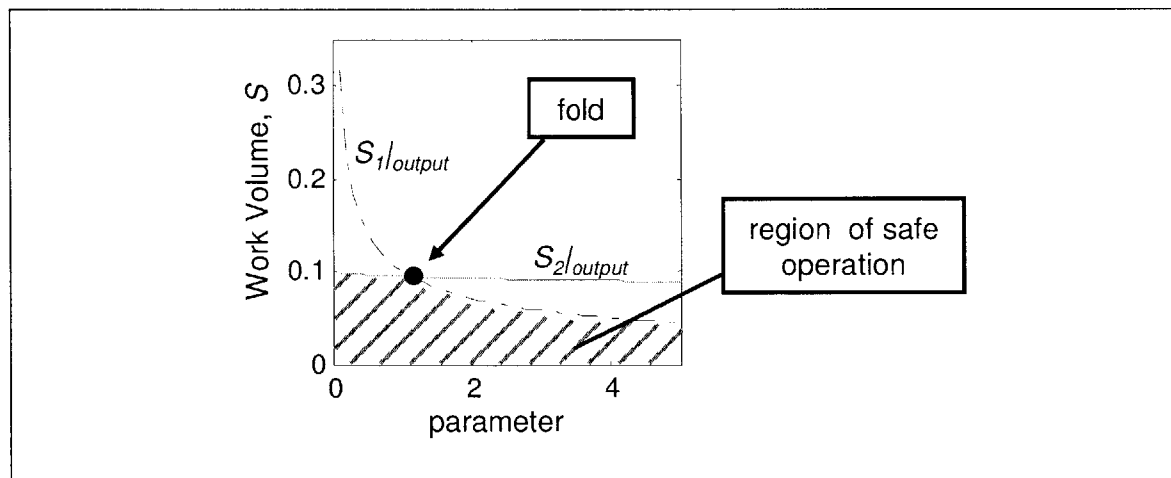
Figure 2.6: *A "fold" in work volume plots is caused by a location change of maximum stress in the mechanism*

One interesting point about work volume plot folds is that they are almost exclusively characterized by a negative second derivative, i.e. folds are concave features. To examine why this is true, a counter example is given in Figure 2.7 to show what would be required to create

the opposite effect. The reason why concave folds are not observed is that $S_i|_{output}$ does not undergo abrupt changes that would appear as folds.
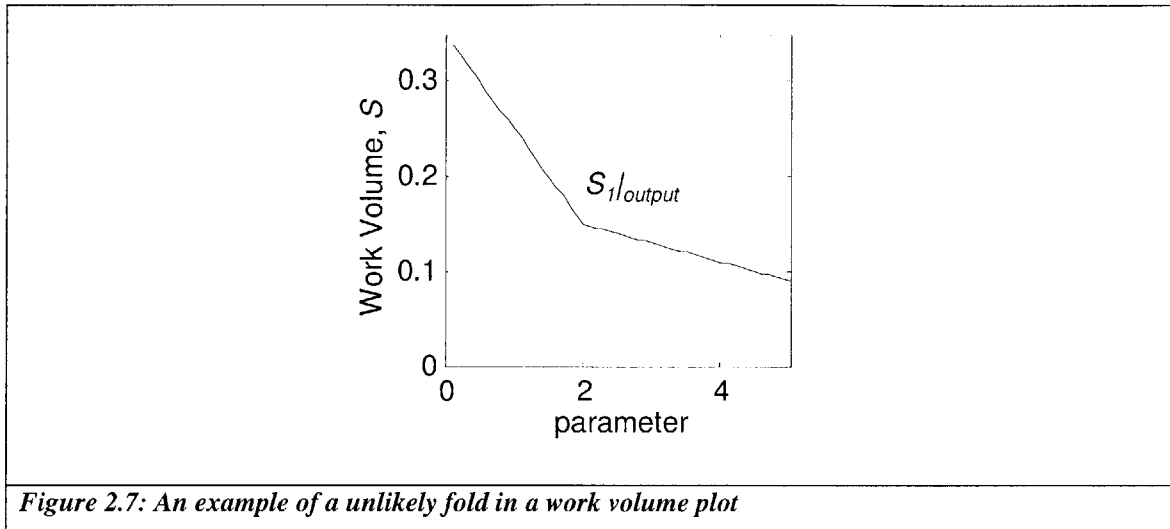
Figure 2.7: An example of a unlikely fold in a work volume plot

At the same time, it is assumed that the scale and resolution of the plots is appropriately chosen to avoid any case where such a feature would be falsely created. An example of what not to do can be explained simply using the model of a cantilever beam. In a cantilever beam where the input is the same as the output, the work volume scales with L^2/h, where L is the length and h is the dimension perpendicular to the neutral axis. If one were to plot the work volume vs. h, one would find it has the relation $1/h$. If inappropriate bounds are placed on the plot (i.e. $L \sim 30$mm and h ranges from 0.75mm to 76mm) one would find a sharp feature near $h \sim 13$mm where the work volume appears to rise suddenly. Plotting work volume using a low resolution on the h axis would give the appearance of a sharp feature that doesn't actually exist.

CHAPTER 3

3 GENERATING VISUAL INFORMATION USING CONVENTIONAL MODELING TECHNIQUES

3.1 Chapter overview

The purpose of this chapter is to explain how to generate 3-D performance data to be converted

into visual format as described in Chapter 2. A flowchart of information flow is given in Figure

3.1. The inputs are the topology, the parameters that described dimensions, and the

inputs/outputs of the mechanism.

Figure 3.1: This chart shows information flow in generating performance data. Performance data are shown within shaded gray boxes.
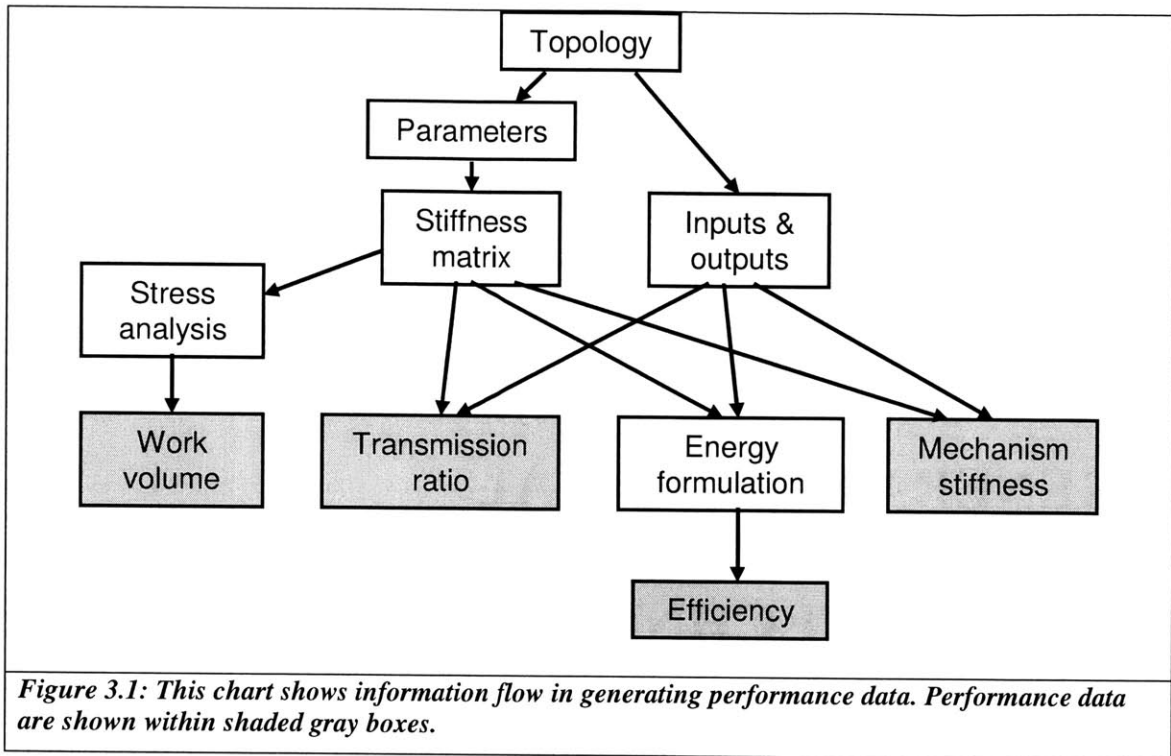
3.2 Fundamental equations

3.2.1 Stiffness matrix, K

The elasto-mechanics of CMs can be modeled using a stiffness matrix. Documentation on the creation of the stiffness matrices used in this thesis for analysis purposes can be found in [4, 21]

The stiffness matrix is used in converting between forces and displacements using the following equation:

$$f = Kx$$

(3.1)

Where f is the applied force vector, K is the global stiffness matrix, and x is the displacement vector of all locations in the mechanism.

3.2.2 Work volume, S

The work volume of a mechanism, qualitatively described in section 2.3.1, may be found in a linear system using Equation 3.2:

$$x_{max} = \frac{\sigma_{allow}}{\sigma_{proof}} K^{-1} f_{proof}$$

(3.2)

Where f_{proof} is any applied actuator force, and σ_{proof} is the maximum stress experienced by the mechanism loaded by f_{proof}.

3.2.3 Energy efficiency, η

The energy efficiency of a mechanism is a ratio of the energy delivered to the output divided by the energy taken in at the input. However, to extract energy from a mechanism, there must be something attached to the output that receives a force carried out over a distance. Two common ways of modeling an output in a linear system are to either add a constant force at the output or to attach a spring that resists motion. The energy extracted by a constant force at the output would be calculated via Equation 3.3:

$$E_{out} = x^T f_{out}$$

(3.3)

Where f_{out} is the force applied at the output. The energy extracted by a spring at the output is given by Equation 3.4:

$$E_{out} = \frac{1}{2} x_{out}^T K_{out} x_{out}$$

(3.4)

55

Where K_{out} is the stiffness matrix for the spring attached to the output, and x_{out} is the displacement at the output. The energy provided at the input is affected by both the output spring and the mechanism stiffness. These can be combined into the same stiffness matrix, which is here called K_T. In general, we are more interested in the spring model of the output because it is a passive model and has no possibility of back-driving the system. In the case of the output modeled as a spring, knowing K_T along with the output stiffness allows a formulation the overall mechanism efficiency, η.

$$\eta = \frac{x_{out}^T K_{out} x_{out}}{x^T K_T x} \tag{3.5}$$

3.2.4 Transmission ratio, Tr

The transmission ratio, Tr, is given by Equation 3.6:

$$Tr = \frac{|x_{out}|}{|x_{in}|} \tag{3.6}$$

However, it is important to note that the transmission ratio for a compliant mechanism is different than that of a non-compliant mechanism because CMs store strain energy. Additionally, the nature of the output affects the transmission ratio because of the finite stiffness of the mechanism's load path from input to output.

3.2.5 Multi-axis vs. single axis compliant mechanisms

Multi-axis CMs are different from single axis CMs in that they have multiple inputs to control the multiple degrees of freedom. One question that arises in a multi-axis system is that of the work volume. In a mechanism with a single input, the work volume is the range of motion of the

output as actuated at the input. In the multi-axis case, this definition still holds, but it must be made more specific by assigning a work volume to each direction of motion of the output. The work volume in a specific direction can be defined as $S| \hat{x}$, where $\hat{x}$ is the direction of the output motion. To obtain range of motion in direction $\hat{x}$ in a system with multiple degrees of freedom, the inverse kinematics of the mechanism must be used.

3.2.6 Visual-based plots

Example design plots for a compliant four-bar mechanism with a rigid coupler bar are given in this section. The purpose of including these plots is to give a concrete example of what they look like. The mechanism is being designed to meet the following requirements and constraints:

	Table 3.1: Functional requirements and constraints
1	$Tr = 2 \pm 0.2$
2	$\eta \geq 0.6$
3	$S \geq 5$mm
4	$K_{out} = 1.8$ N/mm
5	Material = Aluminum (E = 72 GPa, σ_y = 500 MPa)
6	Must fit in a 80mm planar square
7	Out-of-plane beam dimension = 2.5mm
8	In-plane thickness dimensions of beam 1 and 2 are equal

Figure 3.2 describes the system being designed and defines the parameters to be varied.

Figure 3.2: A compliant four-bar mechanism
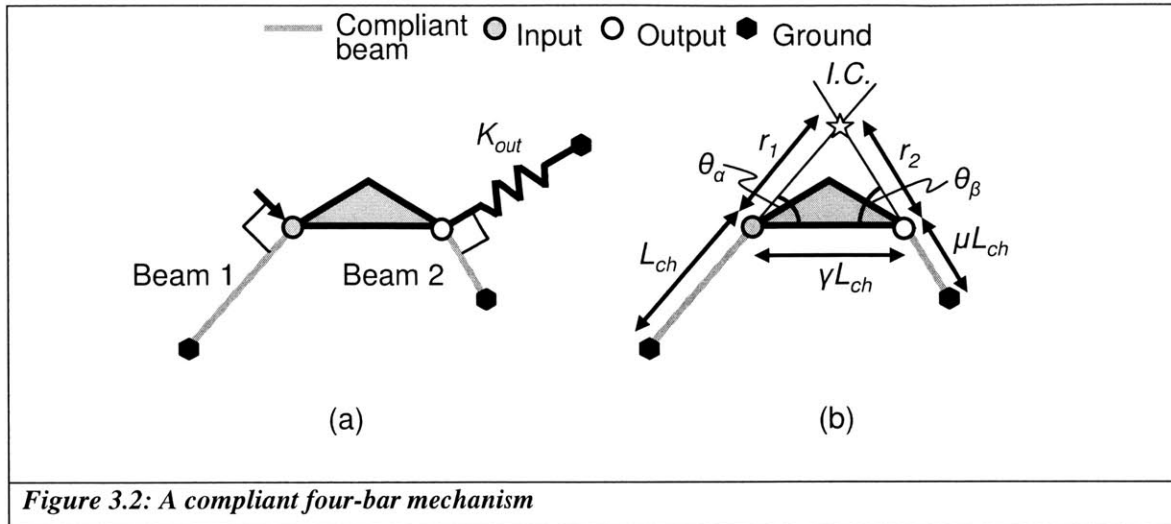
Based on the constraints given above, there are 6 parameters to be varied: L_{ch}, γ, μ, θ_α, θ_β, and h. The variable h, not shown in Figure 3.2, is the in-plane thickness of the beams.

Without any other estimation of size, the golden ratio may be used as a first guess of the characteristic length, L_{ch}, to obtain a value of 50mm. L_{ch} in this case is the length of the first beam, and it is chosen to be as an initial guess. The same rule of thumb can be applied to γ (γL_{ch} = 50mm), and μ can be initially set to 1 (unitless) because the contribution of this parameter to the system is not immediately known. Finally, the thickness of the beams is set to 0.75mm, which approximately the limit of the chosen manufacturing process (in this case, the abrasive water jet). This leaves two parameters to be varied as a starting point for the optimization: θ_α, θ_β. Performance plots for difference values of θ_α and θ_β are shown in Figure 3.3. A 3-D mesh combined with a contour plot provides an efficient method of displaying data. The 3-D mesh is excellent for showing features in the plots, while the contour plot shows lines of iso-performance. Based on trends in the plots, optimization of the four-bar may commence immediately.

Figure 3.3: Compliant four-bar mechanism performance plots
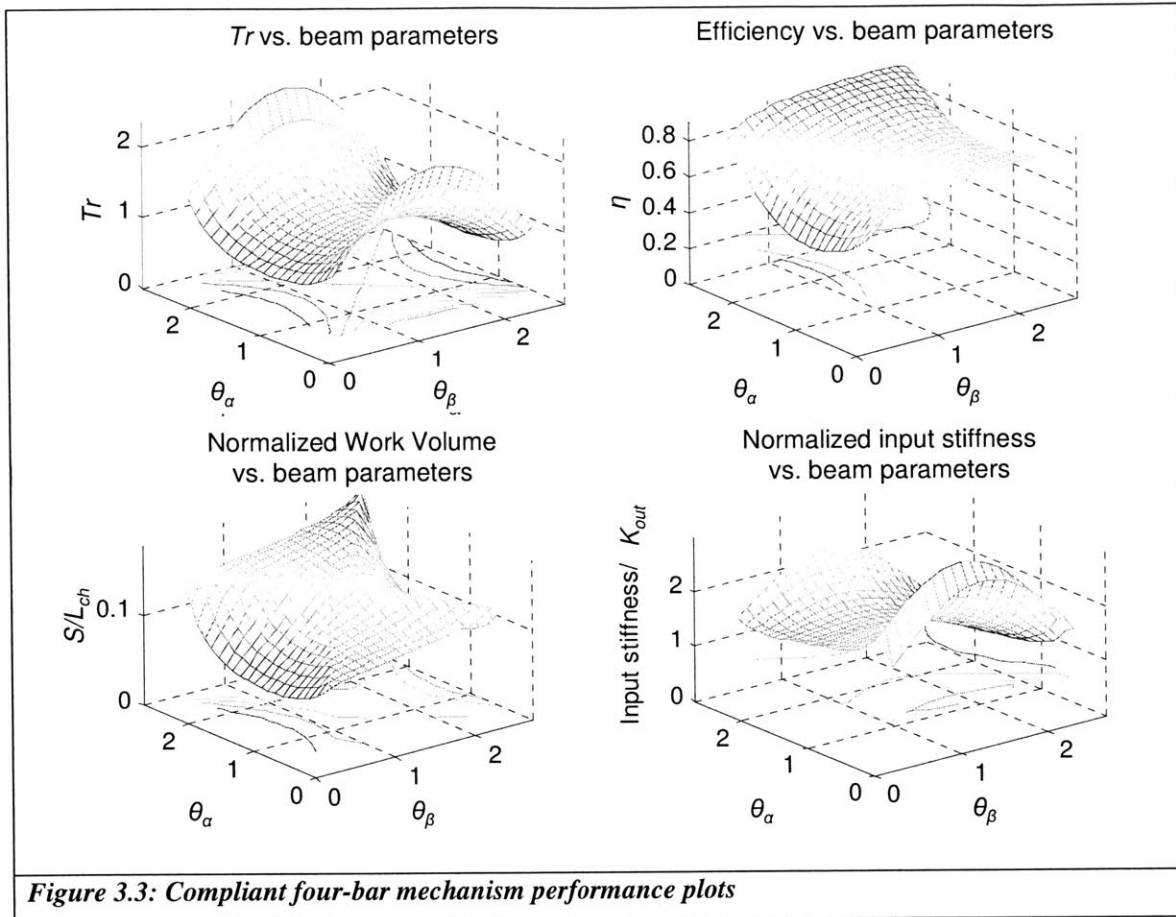
The plots in Figure 3.3 show several details that would be of interest to someone designing a compliant four-bar mechanism. There are minima, maxima, regions of high sensitivity, low sensitivity, and abrupt regions of change between the two. Though a complete optimization is not shown here (see Chapter 5), the reader may gain appreciation for the important design decision driving information that may be contained in such plots.

This page is intentionally left blank.

CHAPTER 4

4 NONDIMENSIONAL MODELING OF COMPLIANT MECHANISMS

4.1 Chapter overview

The purpose of this chapter is to show how CM performance may be nondimensionalized with respect to mechanism parameters. Nondimensionalization is useful for (1) increasing the density of information in performance plots, (2) obtaining a more general optimization tool, and (3) understanding how different non-dimensional parameters interact, which provides more insight into how a particular topology operates. The results of this chapter are:

(A) A nondimensionalized model of a compliant four-bar mechanism. Similar methods may be used to nondimensionalize other compliant mechanisms.

(B) A new model of a beam that is more relevant to instant-center based compliant mechanism design. The new model accurately establishes and describes the relationship between beam

stiffness and instant center location and can be applied to the analysis of other systems with well-defined instant center locations.

(C) A new method of constructing and predicting mechanism stiffness without resorting to stiffness matrices. The new and simple model may be used to perform hand calculations of stiffness and efficiency with error less than 5% when compared to FEA.

In the first part of this chapter, the new model of a beam with modified end conditions will be proposed as a more relevant alternative for instant-center based compliant mechanism design. Next, this model will be used to construct and predict the stiffness of a compliant four-bar mechanism. This stiffness will then be used as a metric for the system as well as a basis for determining mechanism efficiency based on some simple analogies involving mechanical advantage and linear springs. Lastly, the nondimensional form of work volume will be derived from the same equations used to create the beam model.

4.2   Stiffness of a beam with end rotation about a distant point

The motivation for the new model is the low accuracy of current beam models (the fixed-free model and the fixed-guided model) in predicting the stiffness of a compliant-four bar mechanism. In the approach taken in this section, the stiffnesses of two compliant beams are added as if they were springs acting in parallel. However, simply adding the stiffnesses of two compliant beams does not take into account the end conditions of the beams and their associated degrees of freedom. These factors are of great importance to the stiffness of a beam, and current beam models do not accurately capture the end conditions as they occur in CMs.

In CM design where instant center analysis is used, the ends of compliant beams are often connected to rigid bodies whose instantaneous motion can be approximated as rotation about a point (i.e. an instant center). When this end condition is placed upon a compliant beam (i.e. rotation about a point some distance away from the end of the beam), its stiffness is different from that of either a fixed-free beam or a fixed-guided beam. The derivation for the new model with this end-rotation condition is based upon two existing models, from which a general equation for stiffness is obtained. The system of interest is shown in Figure 4.1. Note that the center of rotation lies along the axis of the beam, which is consistent with instant center analysis as it applies to CM design.
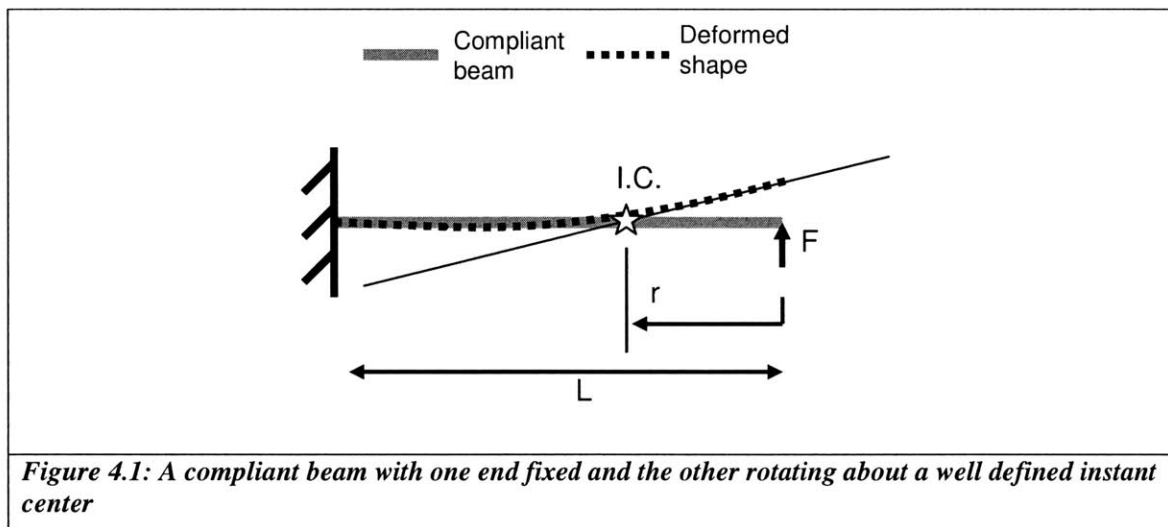
Figure 4.1: A compliant beam with one end fixed and the other rotating about a well defined instant center

The end rotation about the instant center may be difficult to visualize. For clarity, the mechanism may be thought of as a compliant beam with a rigid body connecting the end of the compliant beam to a pin joint at the center of rotation. This is shown in Figure 4.2.
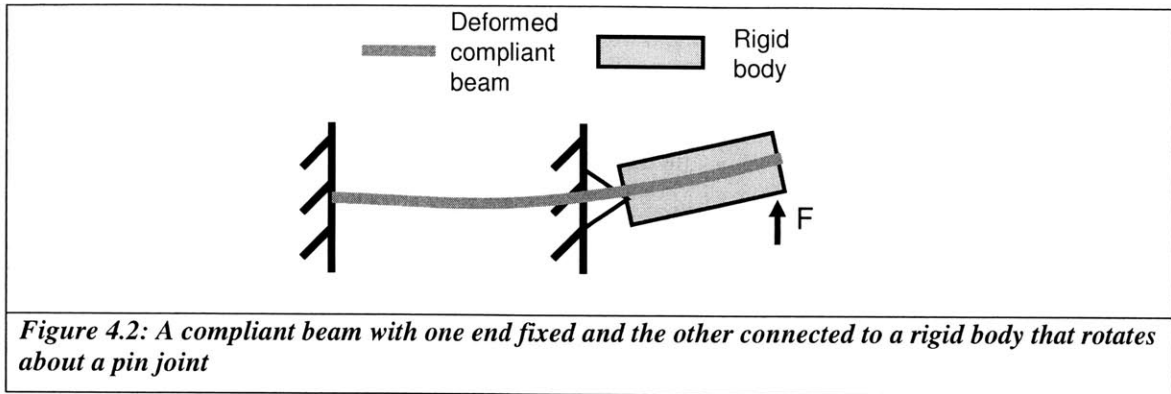
Figure 4.2: A compliant beam with one end fixed and the other connected to a rigid body that rotates about a pin joint
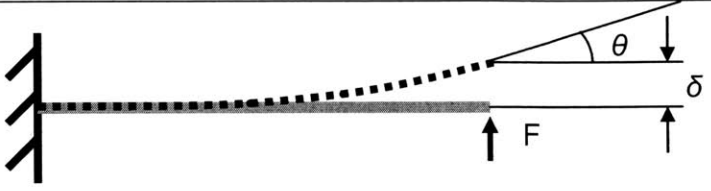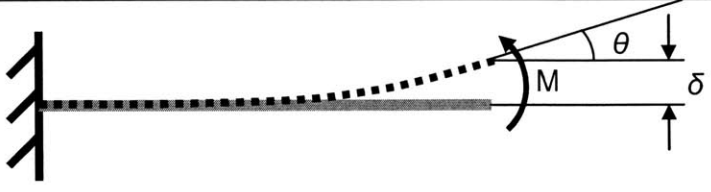
The extra intuition that Figure 4.2 lends is that it is now easier to envision how such an end condition could change the stiffness of the compliant beam, because the rigid body does not comply axially nor does it allow bending across its length.

The stiffness value of interest in this model is $dF/d\delta$. Though the rigid body exerts a moment on the compliant beam, we are only concerned with how the system reacts to external loads, which in turn gives us a measure of stiffness. The internal forces are first found from Equations 4.2 through 4.5, while the forces of interest (external forces) are found in Equations 4.6 to 4.8.

To derive this stiffness, two conventional models are used. These models are shown in Table 4.1.

Table 4.1: The two conventional models used to derive the new model			
Model		δ	θ
		$\dfrac{FL^3}{3EI}$	$\dfrac{FL^2}{2EI}$
		$\dfrac{ML^2}{2EI}$	$\dfrac{ML}{EI}$

However, a third equation must be established to couple these two models. This is the arc-length equation, and it is given by Equation 4.1, where δ and θ are shown in Table 4.1 :

$$\delta = r\theta \qquad (4.1)$$

Equation 4.1 is rearranged to solve for the ratio of θ to δ:

$$\frac{\theta}{\delta} = \frac{1}{r} \qquad (4.2)$$

From the superposition of the above cantilever beam models:

$$\theta = \frac{FL^2}{2EI} + \frac{ML}{EI} \qquad (4.3)$$

$$\delta = \frac{FL^3}{3EI} + \frac{ML^2}{2EI} \qquad (4.4)$$

Solving this set of three equations (4.2, 4.3, and 4.4) for F/δ gives:

65

$$\frac{F}{\delta} = (12 - 6\frac{L}{r})\frac{EI}{L^3}$$

<div align="right">(4.5)</div>

Similarly,

$$\frac{M}{\delta} = (4\frac{L^2}{r} - 6L)\frac{EI}{L^3}$$

<div align="right">(4.6)</div>

Equations 4.5 and 4.6 describe the internal force-displacement and moment-displacement relationships between the compliant beam and the "rigid body." These are necessary to calculate the external forces applied to the system. The external forces are calculated by analyzing the static behavior of the rigid body, shown in Figure 4.3.
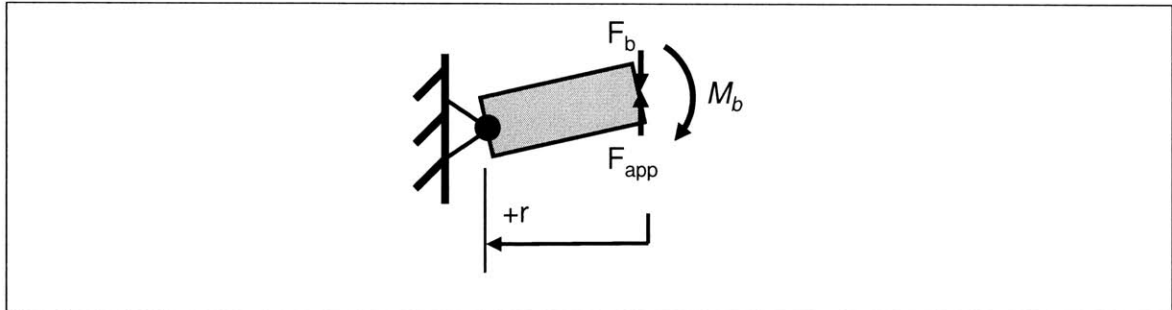
Figure 4.3: Forces acting on the rigid body in the instant center beam model

F_b and M_b are the internal reaction force and moment from the compliant beam shown in Figure 4.2, respectively. F_{app} is the externally applied force. To satisfy static equilibrium, the sum of the moments around the pivot must be zero. Note that the sign of r depends on the position of the pivot relative to the end of the rigid body, as shown in Figure 4.3.

$$\sum M = 0 = F_{app}r - F_b r - M_b$$

<div align="right">(4.7)</div>

Substituting Equations 4.5 and 4.6 into Equation 4.7 (where $F = F_b$ and $M = M_b$), the stiffness of the compliant-beam-rigid-body system is derived.

$$\frac{F_{app}}{\delta} = \left[12 - 12\frac{L}{r} + 4\left(\frac{L}{r}\right)^2\right]\frac{EI}{L^3}$$

(4.8)

In essence, Equation 4.8 relates the stiffness of a compliant beam to the instant center about which the end rotates. Note that as $r \to \infty$, $L/r \to 0$ and the stiffness approaches $12\frac{EI}{L^3}$, which is the same stiffness as that of a fixed-guided beam. Also, when $L/r = 3/2$, the stiffness equals $3\frac{EI}{L^3}$, which is consistent with the end-rotation and stiffness of a fixed-free cantilever beam.

This model is capable of capturing the beam bending behavior with less than 4% error from FEA predictions. The modifier term in front of $\frac{EI}{L^3}$ shall be called the nondimensional stiffness coefficient. For the ith beam in a system, the nondimensional stiffness coefficient is:

$$A_i = 12 - 12\frac{L_i}{r_i} + 4\left(\frac{L_i}{r_i}\right)^2$$

(4.9)

Figure 4.4 shows how the nondimensional stiffness coefficient changes with the ratio L_i/r_i.

Figure 4.4: Nondimensional stiffness coefficient vs. L_i/r_i.
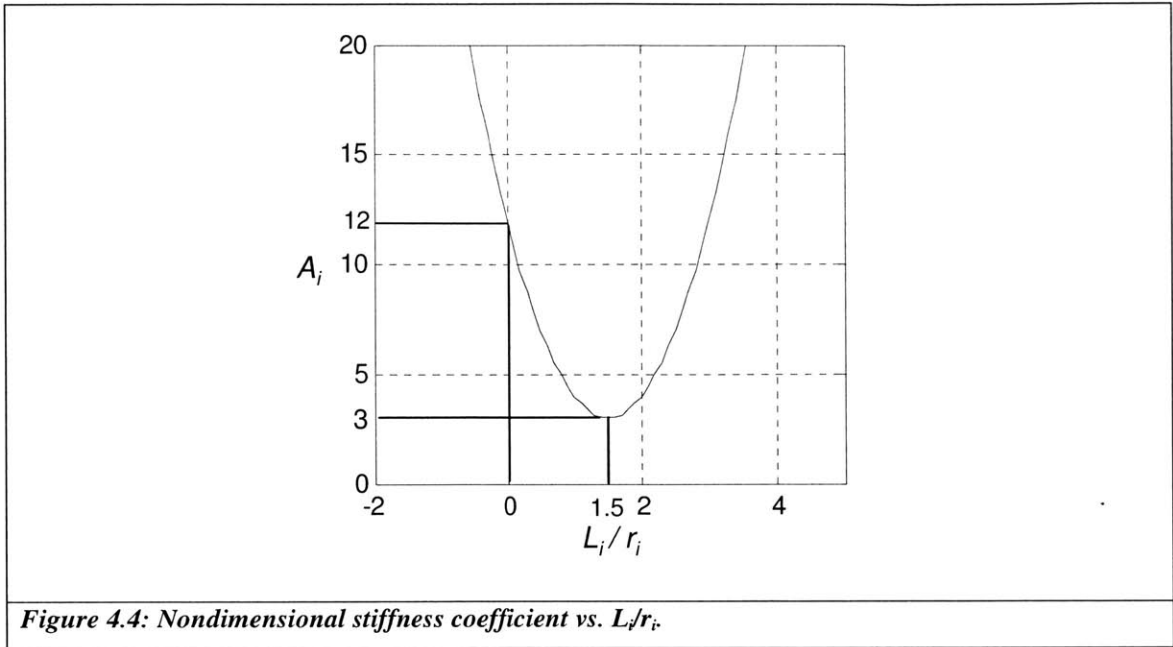
4.3 Constructing mechanism input stiffness

The input stiffness is the derivative of the input force with respect to input displacement. This stiffness is denoted as $K|_{input}$. The effect of a compliant beam, K_1, whose free end is attached to the input is that the stiffness of that compliant is added to $K|_{input}$. Figure 4.5 demonstrates this.
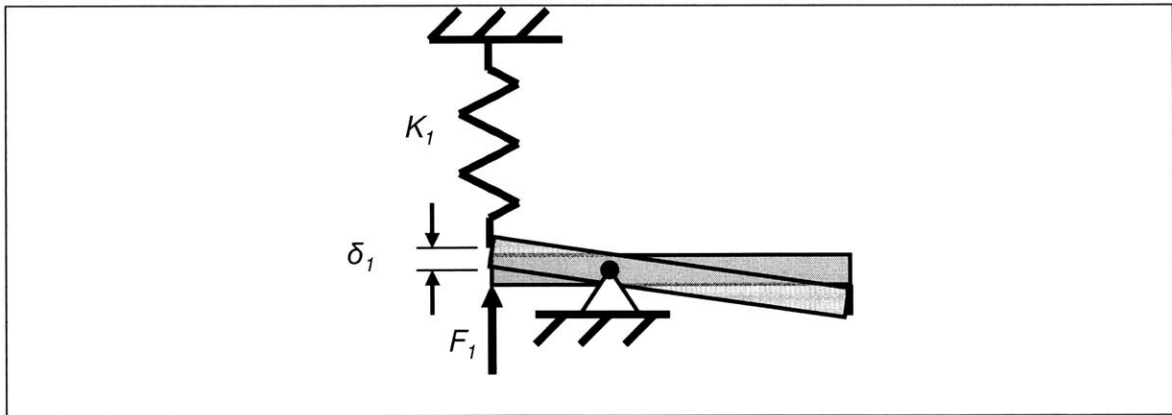
Figure 4.5: A mechanism with a spring attached to the input

In a linear system with small displacements, the behavior of the system in Figure 4.5 is described by Equation 4.10.

$$K_1 = \frac{F_1}{\delta_1}$$

(4.10)

Thus, the input stiffness of the system is:

$$K_1 \big|_{input} = K_1$$

(4.11)

But what is the effect on $K|_{input}$ when adding a second compliant beam to the same rigid body but at a different location? It would have some effect on $K|_{input}$, but that effect is not immediately clear. At this point we move to a simple analogy to explain the effects.

Figure 4.6 shows a rigid lever with a transmission ratio of two and a spring attached to the output. When the lever is displaced, the displacement at the input is half of that of the output, while the force is twice as much at the input. This can be verified by summing the moments at the lever hinge. Figure 4.6b demonstrates the force-displacement relationships and shows that $K|_{input}$ appears as $Tr^2 K_2$ at the input. Note that this is only true when the lever is rigid. When the lever is compliant, additional stiffness terms must be included, though that analysis is left for consideration in future work.
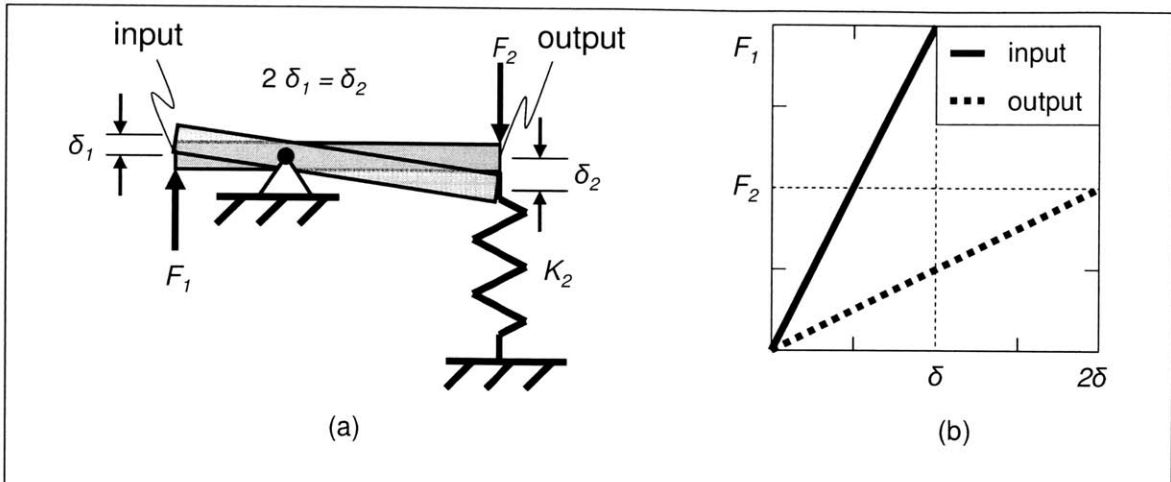
Figure 4.6: The effect of a spring at the output on $K|_{input}$.

Continuing the lever analogy, a mechanism with both a spring at the input and a spring at the

output would appear as in Figure 4.7.
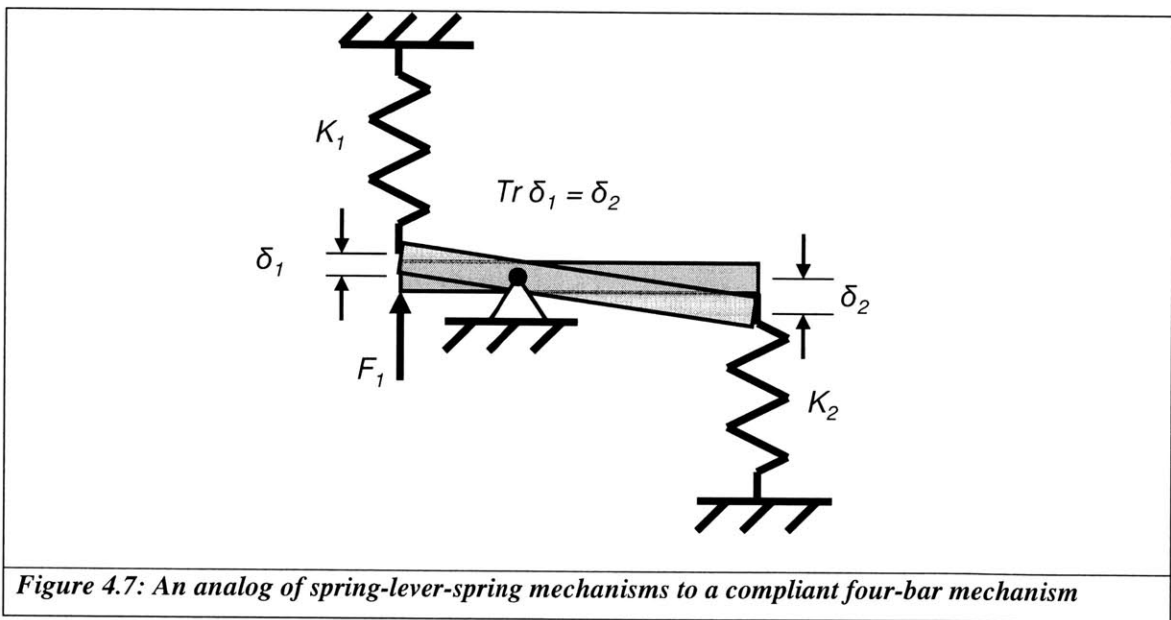
Figure 4.7: An analog of spring-lever-spring mechanisms to a compliant four-bar mechanism

The input stiffness of two springs in parallel appears as:

$$K|_{input} = K_1|_{input} + K_2|_{input} \tag{4.12}$$

$$K|_{input} = K_1 + Tr^2 K_2 \tag{4.13}$$

Equation 4.10 can be used to find the input stiffness of a compliant four-bar mechanism to less than 3% error compared to FEA. The same model could further be used to accurately predict stiffness of a chain of compliant four-bar mechanisms, which make up a majority of single input, single output CMs. Using similar lines of reasoning, the stiffness may be defined at a different point in the mechanism, such as at the output. In this case:

$$K_2 \mid_{output} = K_2 \tag{4.14}$$

$$K_1 \mid_{output} = K_1 / Tr^2 \tag{4.15}$$

The importance and utility of the preceding equation becomes important in the following section.

4.4 Efficiency formulation

The energy efficiency of a linear compliant mechanism may be derived using spring energy equations. The energy transmitted to the output is the energy stored in the output spring.

$$E_{out} = \frac{1}{2} K_{output} \delta_{output}^{\ 2} \tag{4.16}$$

$$E_{in} = \frac{1}{2} K \mid_{input} \delta_{input}^{\ 2} \tag{4.17}$$

K_{output} is the stiffness of the output, i.e. work piece. Equations 4.12, 4.16, and 4.17 combined with the definition of transmission ratio to yields:

$$\eta = \frac{E_{out}}{E_{in}} = \frac{Tr^2 K_{output}}{K_1 + Tr^2 K_{output}} \tag{4.18}$$

71

In the case of the compliant four-bar mechanism defined in Figure 3.2, there are two springs attached at the output: the output spring and the second compliant beam of the four-bar. The second compliant beam adds an additional term to the denominator of Equation 4.18:

$$\eta = \frac{Tr^2 K_{output}}{K_1 + Tr^2 K_2 + Tr^2 K_{output}}$$

(4.19)

It is interesting to note that the Tr^2 terms in the numerator and denominator come from different sources; the Tr^2 in the numerator comes straight out of the ratio of output to input displacement. The Tr^2 terms in the denominator comes from a difference in perceived stiffness due to mechanical and geometric advantage.

To convert the efficiency to nondimensional form, a relationship between K_1, K_2, and K_{output} must be established. Converting between K_1 and K_2 requires analysis of the mechanism's geometry. Looking at Figure 3.2:

$$K_1 = \frac{A_1 EI_1}{L_1^3}$$

(4.20)

The nondimensional numbers A_1 and A_2 can be found from Equation 4.9. The values of r_1 and r_2 can be found in terms of θ_α, θ_β, and γ using the Law of Sines. Assuming that the cross-sections of beams 1 and 2 are equal,

$$K_2 = \frac{A_2 EI_2}{L_2^3} = \frac{A_2 EI_1}{(\mu L_1)^3}$$

(4.21)

4.4.1 Normalization of output stiffness

The term $k = \dfrac{EI_1}{L_1^3}$ is the dimensional force-displacement stiffness term for compliant beams.

This term can be divided out of both equations as described in Equations 4.22 and 4.23.

$$\frac{K_1}{k} = A_1 \tag{4.22}$$

$$\frac{K_2}{k} = \frac{A_2}{\mu^3} \tag{4.23}$$

The choice remains of how the output stiffness should be normalized. The author suggests normalizing the output with respect to the combined mechanism stiffness because then the output scales with the compliant four-bar stiffness, K_{FB}, given in Equation 4.21.

$$K_{FB} = \left(\frac{A_1}{Tr^2} + \frac{A_2}{\mu^3} \right) k \tag{4.24}$$

The normalized output stiffness becomes:

$$\lambda = \frac{K_{output}}{\left(\dfrac{A_1}{Tr^2} + \dfrac{A_2}{\mu^3} \right) k} \tag{4.25}$$

The normalized efficiency becomes:

$$\eta = \frac{\lambda}{1 + \lambda} \tag{4.26}$$

One can now think of efficiency as depending upon the ratio of output stiffness to mechanism stiffness. The efficiency approaches 1 as λ goes to infinity. This is shown in Figure 4.8. The limit as λ approaches infinity must be "taken with a grain of salt," for it relies on the assumption that the load path from input to output is infinitely rigid and stores no strain energy. The degree of accuracy depends on the ratio of the coupler stiffness to the output stiffness. When the coupler is 20 or more times stiffer than the output, the error due to this approximation is less than 5%.
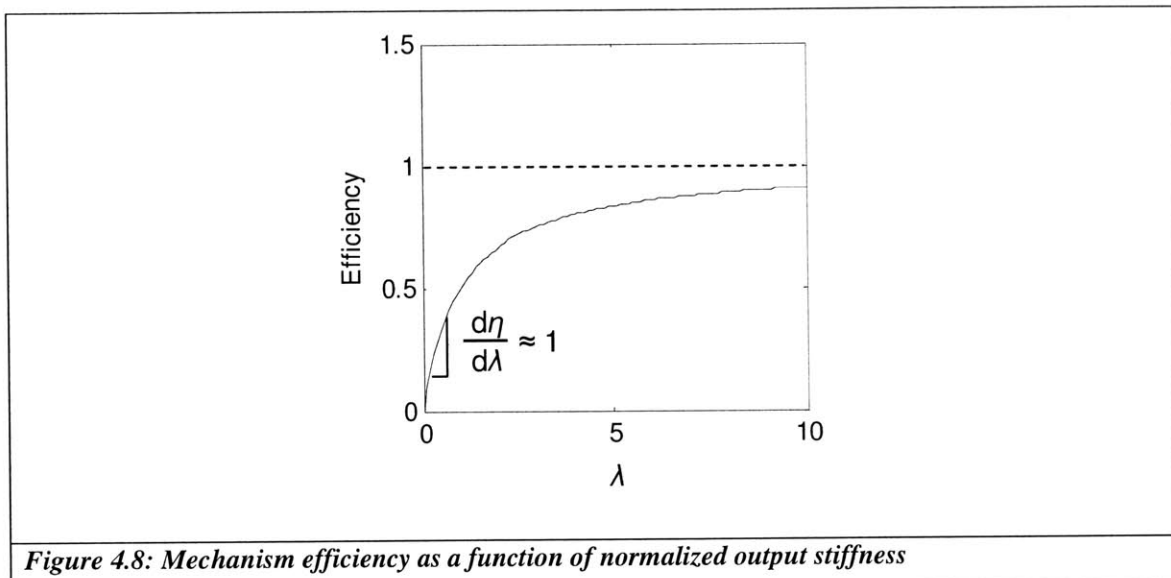
Figure 4.8: Mechanism efficiency as a function of normalized output stiffness

The normalized output stiffness is often not a design parameter of interest, because it may be constrained to a certain value if the nature of the output is well defined in the design problem. A discussion of the selection of nondimensional parameters is given in Section 4.4.2.

4.4.2 Selection of nondimensional parameters

Nondimensional parameters are selected depending on the constraints of the design problem. Variables that are fixed by design constraints become the factors by which other free variables are normalized. As a specific example, if the output stiffness is defined, it no longer makes sense to normalize it with respect to the stiffness of the rest of the mechanism. Instead, one might

choose to normalize other stiffness components (e.g. the stiffness of one of the beams) with respect to the output stiffness. The new efficiency formulation would take on a new form and have new dimensionless variables. The efficiency formulation acts as a quantitative supplement to intuition, or it can act as a source of intuition when intuition is lacking. An example where the output is defined is in the design of compliant grippers, where the work piece is of known (or approximately known) stiffness. Though the current nondimensional model of stiffness cannot account for such a complicated mechanism, improved models would link mechanism efficiency to the stiffness of each component, i.e. compliant element, which could be normalized to the known work piece stiffness. This normalization would show which compliant elements have the greatest effect on mechanism efficiency, which would gives the designer valuable information about which components have the largest impact on performance.

Some variables cannot be used as nondimensional parameters, notably, A_i. The reason is that A_i is not directly correlated to any specific mechanism parameter. Rather, it is function of several mechanism parameters and cannot easily be back-solved (refer to Equation 4.9).

0 lists some relevant nondimensional parameters that can be used in formulating the efficiency. Using these parameters enables a level of abstraction that relates performance to mechanisms of identical shape and proportions, but does not necessarily look at the performance of a mechanism with a particular dimensional value.

Table 4.2: Nondimensional parameters useful for calculating efficiency	
1	θ_α
2	θ_β
3	M
4	γ
5	L/h
6	Tr

Designers would use dimensional mechanism parameters when less abstraction is desired, e.g. when finding actual dimensions of a particular mechanism to meet performance requirements.

4.5 Work volume formulation

This section describes how nondimensional work volume can be formulated for a compliant four-bar mechanism. The stresses in a compliant beam have the following sources:

$$\sigma_{total} = \sigma_{axial} + \sigma_{shear} + \sigma_{bending} \tag{4.27}$$

The displacement of the end also has several sources:

$$\delta_{total} = \delta_{axial} + \delta_{shear} + \delta_{bending} \tag{4.28}$$

To simplify analysis, a few assumptions are made. Axial and shear effects are assumed to be small compared to those of bending. In many CMs, stresses due to axial and shear forces are generally much lower than bending stresses (<5%). Equation 4.29 describes conditions under which shear stresses are small. Equations 4.30 and 4.31 describe conditions under which axial stresses are small. These assumptions remove terms that are insignificant under the majority of cases. Ignoring axial and shear terms maintains generality for a majority of practical four-bar

mechanisms. Other cases not accounted for include those when large loads are being transferred due to high output stiffness ($\lambda > 100$), or short or thin beams are used (in which cases axial and shear terms become relevant). Shear and axial stresses are small in the compliant four-bar of Figure 3.2 under the following conditions:

$$L_{ch}/h, \; \mu L_{ch}/h > 10 \tag{4.29}$$

$$\pi/6 < \theta_\alpha, \; \theta_\beta < 5\pi/6 \tag{4.30}$$

$$7\pi/6 < \theta_\alpha, \; \theta_\beta < 11\pi/6 \tag{4.31}$$

Also, beam buckling is not accounted for because buckling is nonlinear and its inclusion is beyond the primary scope of this thesis. Buckling effects would be prominent in mechanisms with compliant members subjected to high compressive forces. The remaining term in both the displacement and stress equations is the contribution due to bending effects.

4.5.1 Stress calculations

Bending effects arise both from moment and force end-loading of the beams. The stress due to these loads is:

$$\sigma_i = \frac{F_i L_i c_i}{I_i} + \frac{M_i c_i}{I_i} \tag{4.32}$$

From Equations 4.5 and 4.6, the relation between the internal force and moment F and M is found to be:

$$M = F \frac{\left(\dfrac{r_i L_i}{2} - \dfrac{L_i^2}{3} \right)}{\left(\dfrac{L_i}{2} - r_i \right)} \tag{4.33}$$

The range of motion of a beam subject to these loading conditions is found by combining Equations 4.7, 4.8, 4.32 and 4.33:

$$\delta_{max} = \frac{\sigma_y}{E}\frac{L_i^2}{h_i}\frac{\left(4L_i^2 - 12L_i r_i + 12r_i^2\right)}{A_i\left(3r_i^2 - L_i r_i\right)}$$

(4.34)

The parameter r_i is also a function of the rigid coupler length, γL_{ch}. Therefore, the dimensionless work volume is:

$$\frac{S_i}{L_i} = \frac{\sigma_y}{E}\frac{L_i}{h_i} g_i(r_i, L_i)$$

(4.35)

Where

$$g_i(r_i, L_i) = \frac{\left(4L_i^2 - 12L_i r_i + 12r_i^2\right)}{A_i\left(3r_i^2 - L_i r_i\right)}$$

(4.36)

A_i is a function of L_i and r_i and is given in Equation 4.7. The work volume equation must now be extended to include a two-beam system, i.e. include the second beam in the four-bar mechanism. The work volume of beam two measured at the output is $S_2|_{output}$.

$$\frac{S_2|_{output}}{L_{ch}} = \frac{\sigma_y}{E}\frac{\mu^2 L_{ch}}{h} g_2$$

(4.37)

The work volume of the beam at the output is different than at the input due to the transmission ratio. The relation is:

$$S_j\big|_{output} = S_j\big|_{input} Tr \tag{4.38}$$

Therefore,

$$\frac{S_j\big|_{output}}{L_{ch}} = Tr \frac{\sigma_y}{E} \frac{L_{ch}}{h} g_1 \tag{4.39}$$

The work volume of the mechanism is the minimum of all the work volumes evaluated at the output.

$$\frac{S\big|_{output}}{L_{ch}} = \min\left(\frac{S_1\big|_{output}}{L_{ch}}, \frac{S_2\big|_{output}}{L_{ch}} \right) \tag{4.40}$$

To obtain a simpler form of work volume, it is assumed that:

$$g_1 \approx g_2 \tag{4.41}$$

The validity of Equation 4.35 is discussed further in Section 4.5.2. This assumption reduces the comparison of work volumes evaluated at the output to a comparison between Tr and μ^2, because the other terms of the work volume equations are equal and cancel out. The ratio of μ^2/Tr becomes a predictive tool for determining which beam will fail first, i.e. limit the system's work volume. The ratio μ^2/Tr can be thought of as the ratio of the range of motions of beam two to beam one as evaluated at the output. If $\mu^2 > Tr$, beam one becomes the limiting factor because its work volume evaluated at the output is smaller and vice versa. This intuitive relationship can be extracted from the equations below:

$$\frac{\mu^2}{Tr} > 1, \text{ then } \frac{S|_{output}}{L_{ch}} = Tr\frac{\sigma_y}{E}\frac{L_{ch}}{h}g_1 \tag{4.42}$$

$$\frac{\mu^2}{Tr} < 1, \text{ then } \frac{S|_{output}}{L_{ch}} = \frac{\sigma_y}{E}\frac{\mu^2 L_{ch}}{h}g_2 \tag{4.43}$$

$$\frac{\mu^2}{Tr} = 1, \text{ then } \frac{S|_{output}}{L_{ch}} = Tr\frac{\sigma_y}{E}\frac{L_{ch}}{h}g_1 = \frac{\sigma_y}{E}\frac{\mu^2 L_{ch}}{h}g_2 \tag{4.44}$$

Figure 4.9 shows the nondimensional work volume of the compliant four-bar mechanism plotted against the nondimensional values μ^2/Tr and L/h. The parameters used in the compliant four-bar mechanism (Figure 3.2) are given in Table 4.3.

Table 4.3: Parameters used in creating Figure 4.9	
θ_α	$\pi/2$
θ_β	$\pi/2$
w	0.75mm
γ	1

Figure 4.9 was generated from equation 4.40, and it matches with FEA to within 4% for the conditions described in section 4.5.2. A fold (see section 1.3.2) in the surface plot occurs where $\mu^2/Tr = 1$, indicating the accuracy of the yield criterion μ^2/Tr. Figure 4.9 also shows that S/L is only weakly dependent upon μ^2/Tr when $\mu^2/Tr > 1$. This makes intuitive sense, because beam one contributes the limiting range of motion above this value, so increasing the range of motion of beam two has no effect on the overall work volume of the system. When $\mu^2/Tr < 1$, work volume is linearly dependent upon μ^2/Tr, which is an effect that can also be extracted from the equations. S/L is positively dependent upon L/h over all values. This also makes intuitive sense, as increasing L/h increases both beam dimensions, which always increases the work volume.

Figure 4.9: Nondimensional range of motion vs. beam parameters: a fold occurs at $\mu^2/Tr = 1$
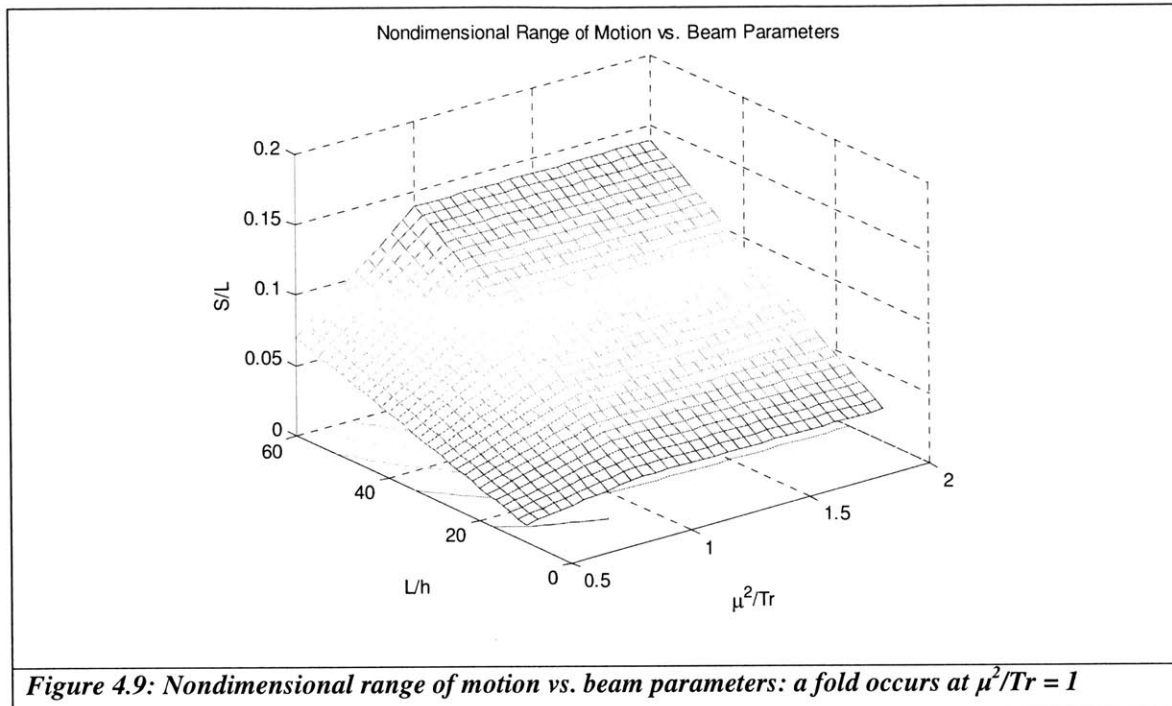
4.5.2 Discussion of assumptions

The assumption of Equation 4.35 adds error to the model. The error due to this assumption is less than 10% for the conditions in Table 4.4:

Table 4.4: Values of θ_α and θ_β for which the given assumption is valid with less than 10% error		
Condition	Values	Picture
1	$\dfrac{\pi}{4} < \theta_\alpha, \theta_\beta < \dfrac{3\pi}{4}$	
2	$\theta_\alpha = \theta_\beta$	
3	$\theta_\beta = \pi - \theta_\alpha$	
4	$\theta_\beta = 2\pi - \theta_\alpha$	

The error is small for condition 1 because for angles in the range [$\pi/4$, $3\pi/4$], the ratio of L_f/r_i is small, which makes the work volume modifier g insensitive in that range. Conditions 2 through 4 give error on the order of 3% because the stiffness coefficients, g's, are equal or close to equal.

Should the parameter values θ_α and θ_β not meet one of the conditions in Table 4.4, the work volume modifiers g_1 and g_2 cannot be dropped when determining which beam fails. Instead, g_1 and g_2 must be included, making the relevant nondimensional number where the beams have equal stresses $g_2\mu^2/g_1 Tr$. Using $g_2\mu^2/g_1 Tr$, the location of the fold with respect to θ_α and θ_β can be predicted within 10% of FEA for the following values of θ_α and θ_β:

$$\pi/6 < \theta_\alpha, \theta_\beta < 9\pi/20 \tag{4.45}$$

$$11\pi/20 < \theta_\alpha, \theta_\beta < 19\pi/20 \tag{4.46}$$

$$21\pi/20 < \theta_\alpha, \theta_\beta < 29\pi/20 \tag{4.47}$$

$$31\pi/20 < \theta_\alpha, \theta_\beta < 11\pi/6 \tag{4.48}$$

4.6 Transmission ratio

The transmission ratio for a four-bar with a rigid coupler link is dependent upon only two parameters: θ_α and θ_β. Instant center analysis can be applied to the four-bar shown in Figure 3.2. Using the Law of Sines, the ratio r_2/r_1 becomes $\sin(\theta_\alpha)/\sin(\theta_\beta)$. For other mechanisms involving finite stiffness along the input-output load path, instant center analysis alone is not sufficient to determine the transmission ratio. The reason is that added compliance in members assumed to be rigid makes instant centers less well-defined. Transmission ratios can be found from instant centers only when their accurate location is known. Thus, compliance in "rigid" members reduces the accuracy of that analysis.

This page is intentionally left blank.

CHAPTER 5

5   CASE STUDY AND HYPOTHESIS CONFIRMATION

5.1   Chapter Overview

The purpose of this chapter is to prove hypotheses one and two found in Section 1.6 of this thesis

through the use of an example optimization scenario (hypotheses three and four were discussed

in Chapters 4 and 2, respectively). Hypothesis one is confirmed using visual-based methods

(VBMs) to optimize a simple CM and show sensitivity data.

$$\text{Number of plots} < N*P/2 \tag{5.1}$$

Satisfying Equation 5.1 for a particular CM validates hypothesis two by example. N is the

number of parameters, and P is the number of performance metrics.

The MATLAB code used in this optimization is documented in the appendix.

5.2 Optimization of a simple compliant mechanism

5.2.1 Problem definition

Figure 5.1 shows the topology of the mechanism being optimized.
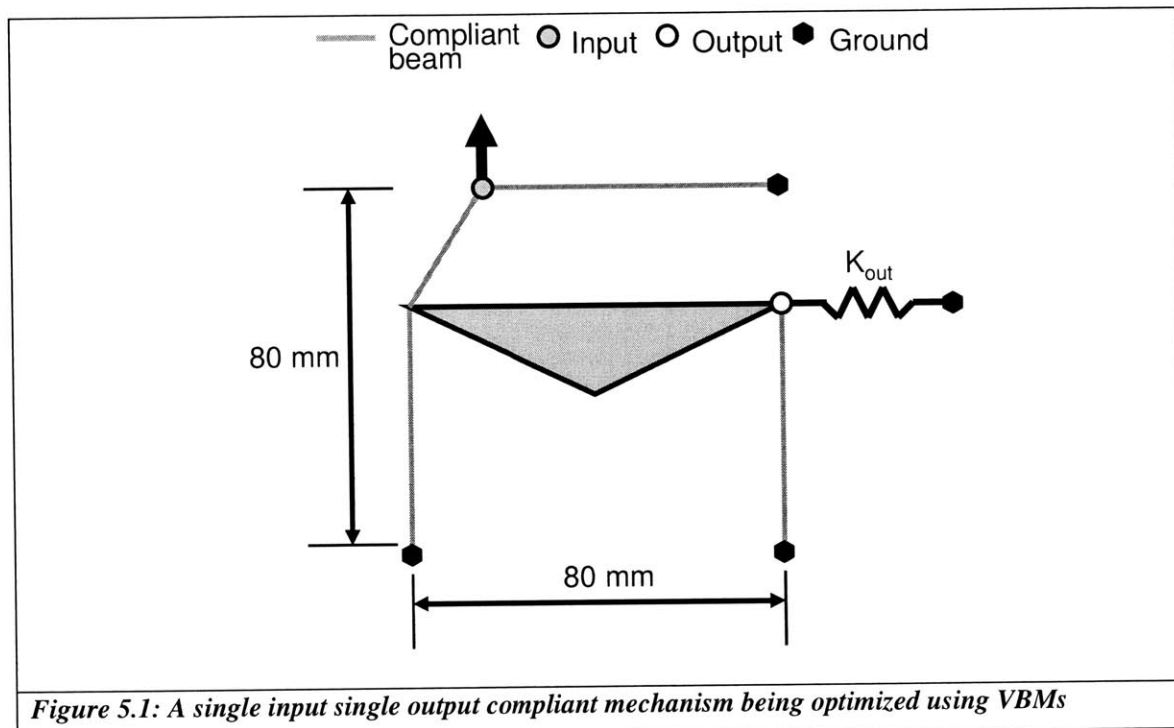
Figure 5.1: A single input single output compliant mechanism being optimized using VBMs

The mechanism receives a vertical input along the upper edge of the design space (an 80mm x 80mm square), though the exact location is variable (i.e. able to be changed). The output is horizontal, linear, and lies along the right side of the design space. The work piece at the output has a spring constant of 1.8N/mm. The mechanism is to have a transmission ratio of 2 ± 0.1, a work volume greater than 2.5mm, and an energy transmission efficiency greater than 30% (and as high as possible). The mechanism is of uniform out-of-plane thickness and the lower bound is 1.6mm. The functional requirements are summarized in Table 5.1, and the constraints in Table 5.2.

Table 5.1: Functional requirements	
1	Transmission ratio = 2 ± 0.1
2	Work volume > 2.5mm
3	Energy efficiency > 30%

Table 5.2: Design constraints	
1	Output stiffness = 1.8 N/mm
2	Design space = 80mm x 80mm
3	Uniform mechanism depth > 1.6mm
4	Compliant beam thickness > 0.75mm
5	Vertical input force along upper edge of design space
6	Horizontal and linear output displacement along right edge of design space

5.2.2 Parameter definition

Figure 5.2 shows the important dimensions that are to be optimized.
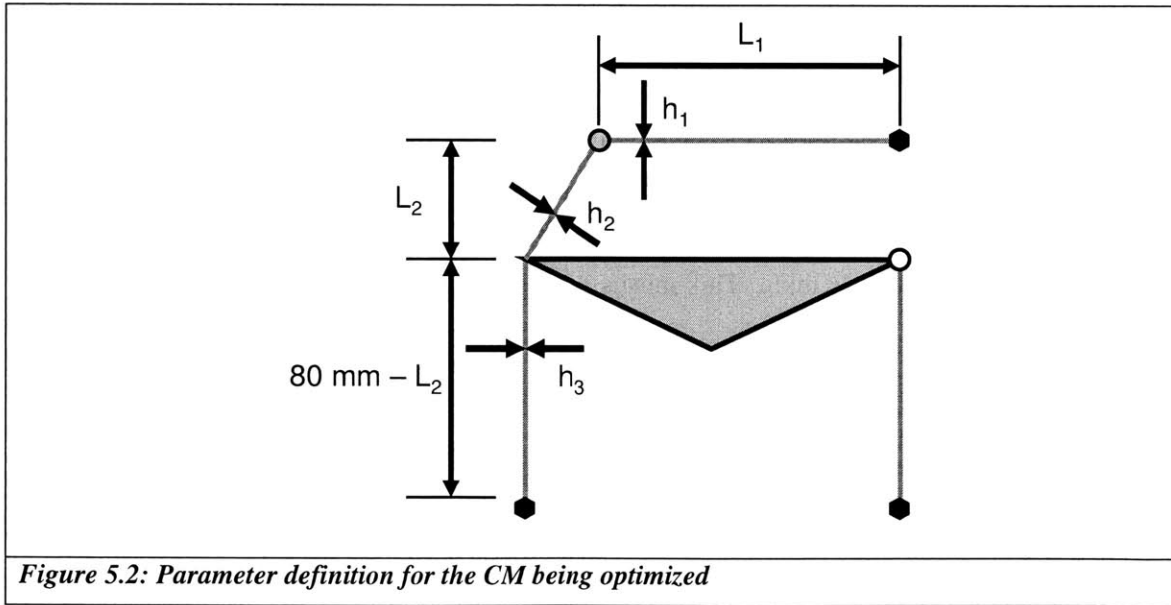
Figure 5.2: Parameter definition for the CM being optimized

The minimum number of parameters is chosen that still preserves the intent of the design. Minimizing the number of parameters limits the size of the design space, which reduces the number of plots that must be created and interpreted to approach an optimum solution. This also

reduces the time required to optimize a mechanism. Without design intent, the model in Figure 5.1 could require many parameters ($\geq$20) to describe the dimensions. However, with design intent incorporated into the model the number of critical parameters can be reduced to 6. Table 5.3 shows information about the design intent.

Table 5.3: A list of the important design intent information contained within Figure 5.1 and Figure 5.2	
1	The entire mechanism is of uniform out-of-plane thickness
2	The four-bar coupler is considered to be infinitely rigid
3	The compliant element along the top is horizontal
4	The locations where the mechanism is grounded remain as shown
5	The four-bar's compliant elements are parallel, vertical, and of equal length and thickness

The number of plots needed to display all of the information is $N*P/2$, where N is the number of parameters and P is the number of relevant performance metrics. In general, it is desirable to reduce the number of parameters because this reduces the number of required plots and the time required to complete the optimization process. The reduction of P is accomplished through logical incorporation of design intent, which is left to the judgment of the designer. Here N has been reduced to six, while P is three. This means nine plots are required to inspect the design space and optimize the mechanism.

5.2.3 Optimization strategy

The values of L_1 and L_2 are of greatest concern initially – the beam thicknesses (h_1, h_2, and h_3) can be set to the minimum value of 0.75mm (the limit of the MIT PCS Laboratory's manufacturing process). Minimizing the thickness as an initial guess also minimizes mechanism stiffness while increasing the work volume. However, the performance sensitivity must be checked later to verify that the mechanism performance will not fall outside requirements given

the tolerances on fabrication. Additionally, the out-of-plane thickness is set to its minimum value (1.6mm) to maximize the compliance of the structure in the direction of motion.

5.2.4 Visual plots used

With the design intent captured in mechanism parameters, optimization using plots may begin. Figures 5.3 through 5.9 map out the design space for the parameters L_1, L_2, h_1, h_2, h_3, and b, where b is the out-of-plane thickness of the mechanism.

Figure 5.3 through Figure 5.9 show a common region that satisfies all the functional requirements. Values of L_1 = 70mm and L_2 = 32mm are chosen because they maximize the work volume and efficiency. These two parameters are not sensitive to dimensional changes due to for instance fabrication or assembly.
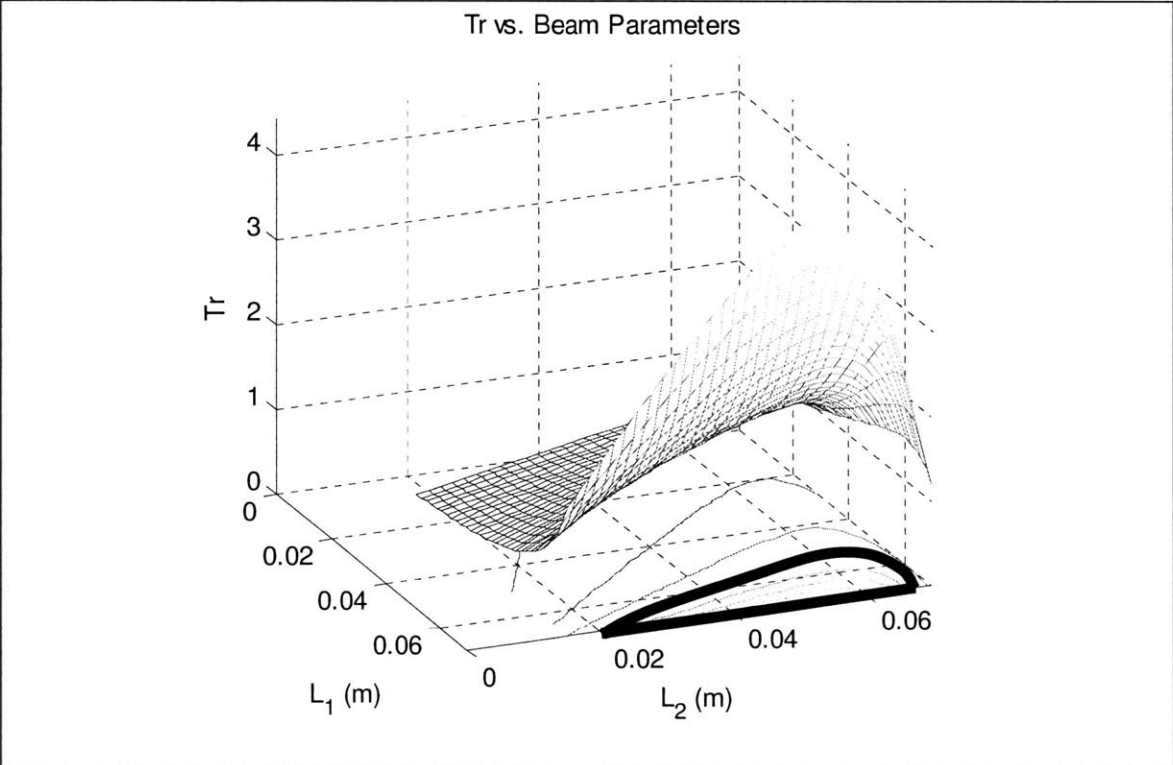
Figure 5.3: Transmission ratio vs. L_1 and L_2

Figure 5.4: Efficiency vs. L₁ and L₂
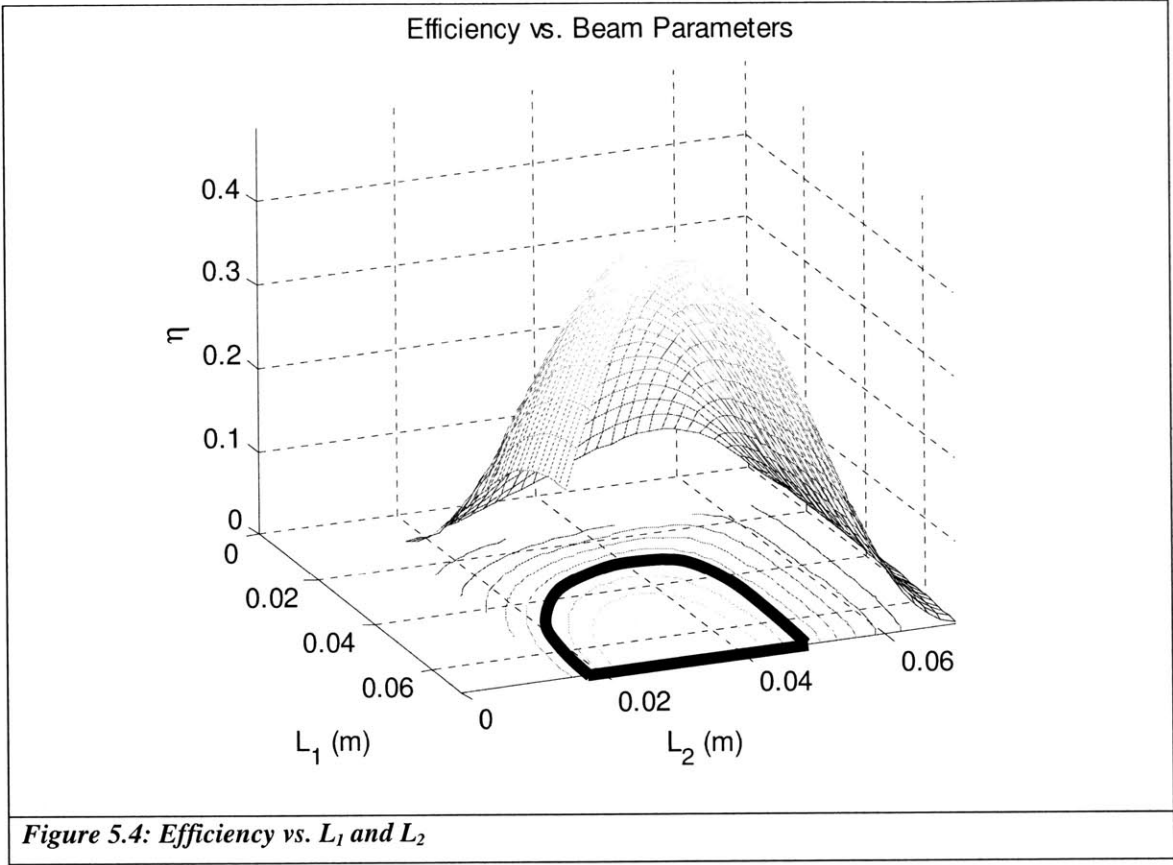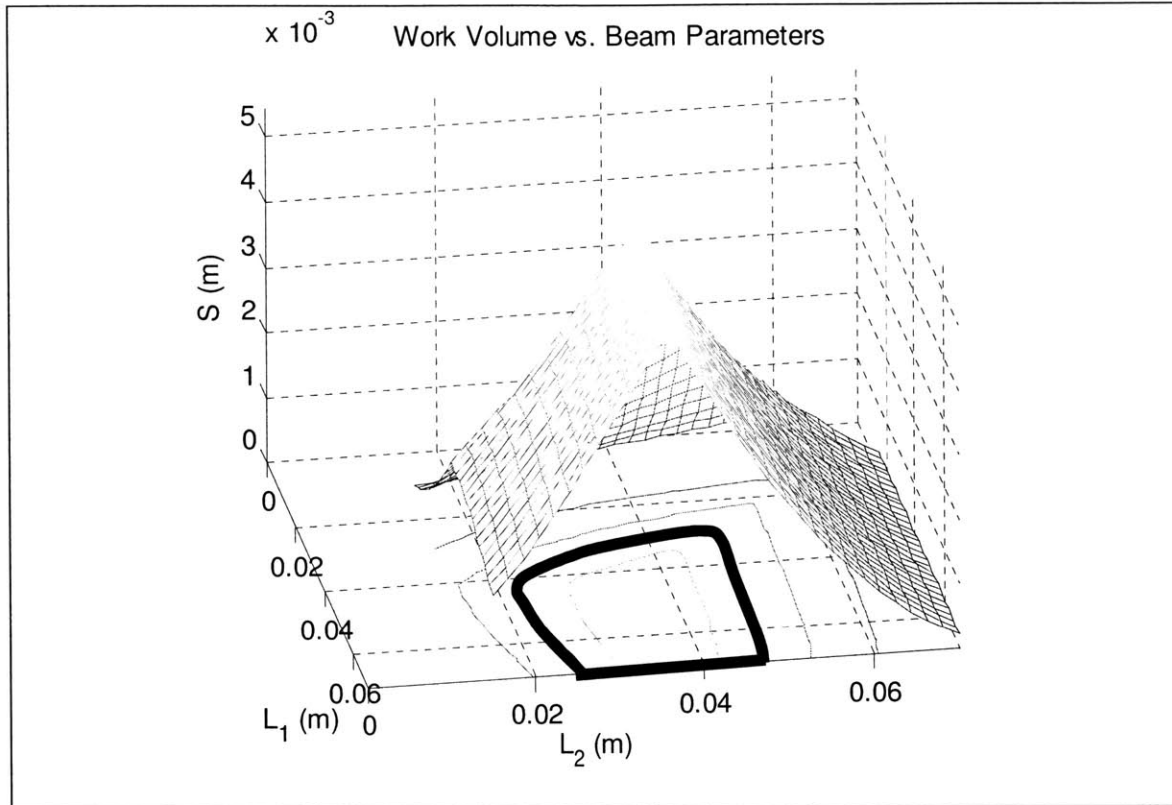
Figure 5.5: Work volume vs. L_1 and L_2

Next, two thickness values, h_1 and h_2, are optimized using the chosen values for L_1 and L_2. The

transmission ratio is not shown for these two variables because Tr does not change more than

0.01 across the range of h_1 and h_2 values specified in the figures. The important thing to note in

Figure 5.6 and Figure 5.7 is that the performance at $h_1 = 0.75$mm and $h_2 = 0.75$mm remains

within acceptable bounds (i.e. within the area surrounded by the black line) for manufacturing

tolerances of 0.125mm, which are determined by the selected manufacturing process. In other

words, the point of operation lies in the center of the area of tolerance, and the area of tolerance

lies completely within the area of acceptable performance. The area of tolerance is defined here

as the area surrounding the desired point of operation (i.e. $h_1 = 0.75$mm and $h_2 = 0.75$mm) whose

outer edges are determined by the manufacturing tolerance.

Efficiency vs. Beam Parameters

Point of
operation

Area of
acceptable
performance

Area of
tolerance

Figure 5.6: Efficiency vs. h₁ and h₂

Work Volume vs. Beam Parameters

Point of
operation

Area of
acceptable
performance

Area of
tolerance

Figure 5.7: Work volume vs. h₁ and h₂
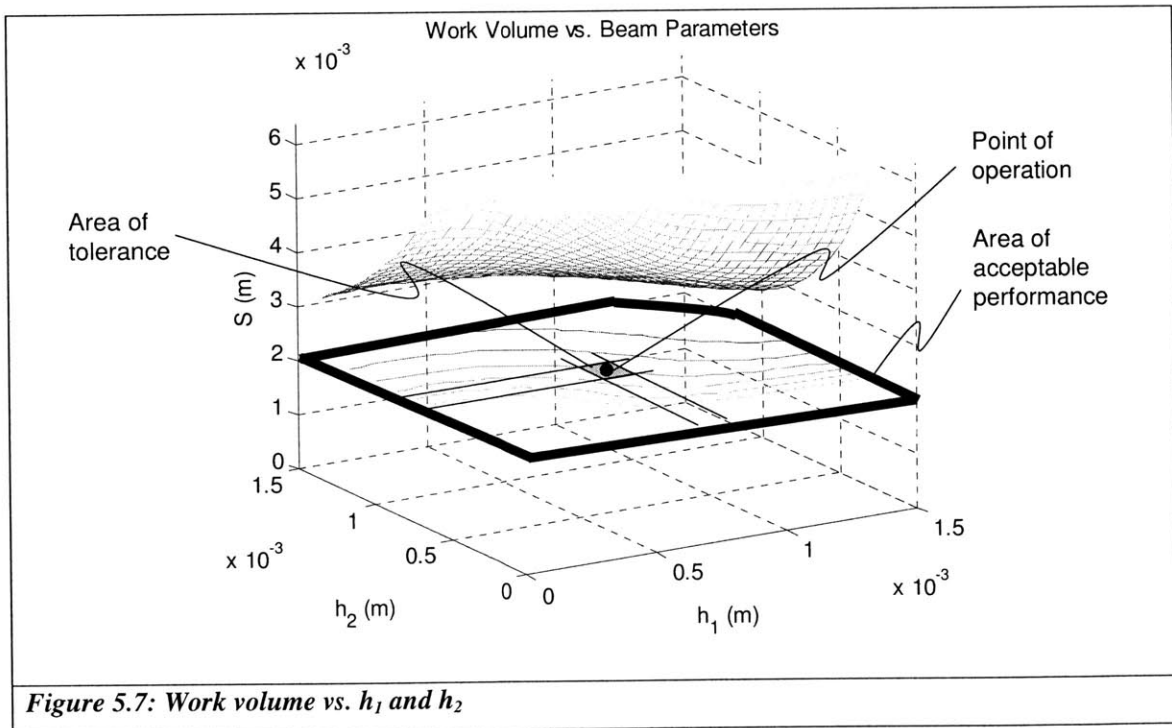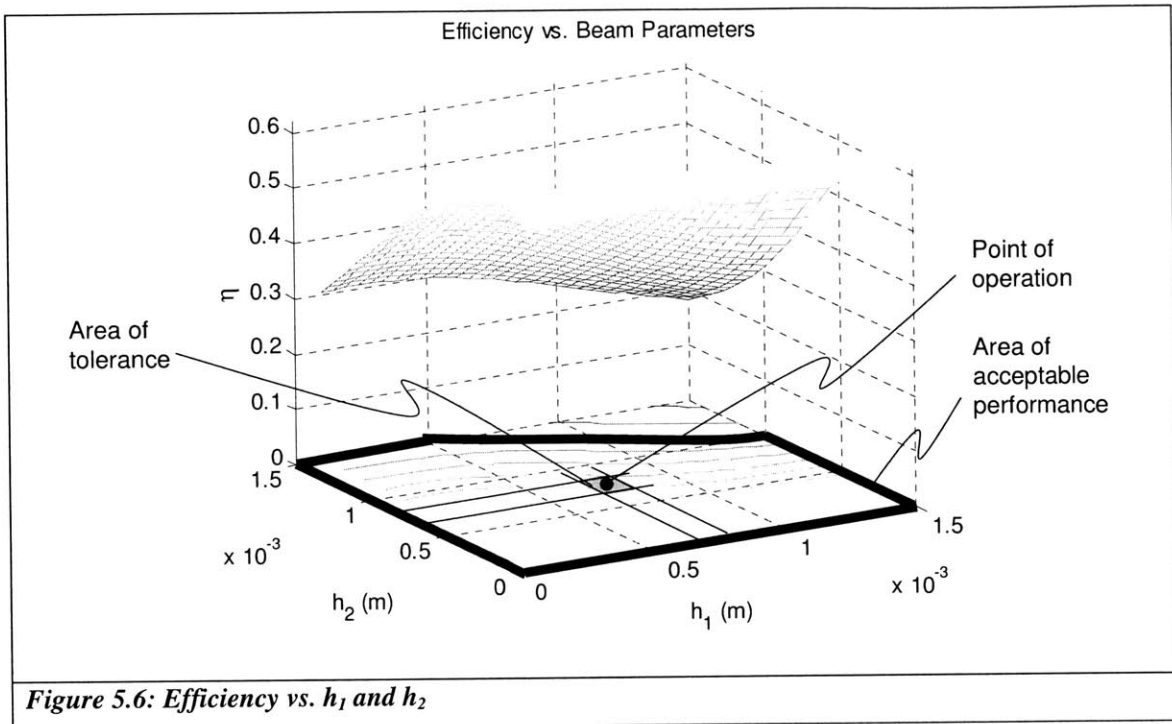
The remaining two parameters, h_3 and b, are used create Figure 5.8 and Figure 5.9. Again, the performance remains within acceptable bounds for hypothetical manufacturing tolerances for h_3 = 0.75mm and b = 1.6mm.
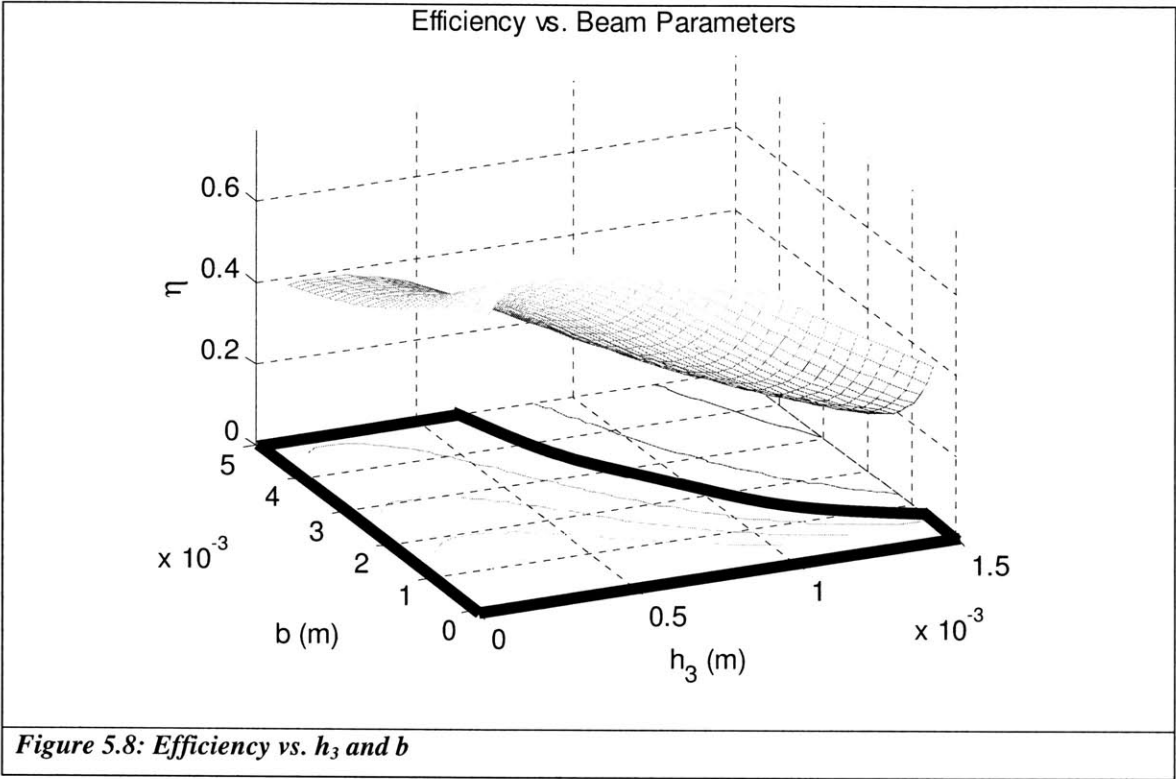
Figure 5.8: Efficiency vs. h_3 and b

Figure 5.9: Work volume vs. h₃ and b
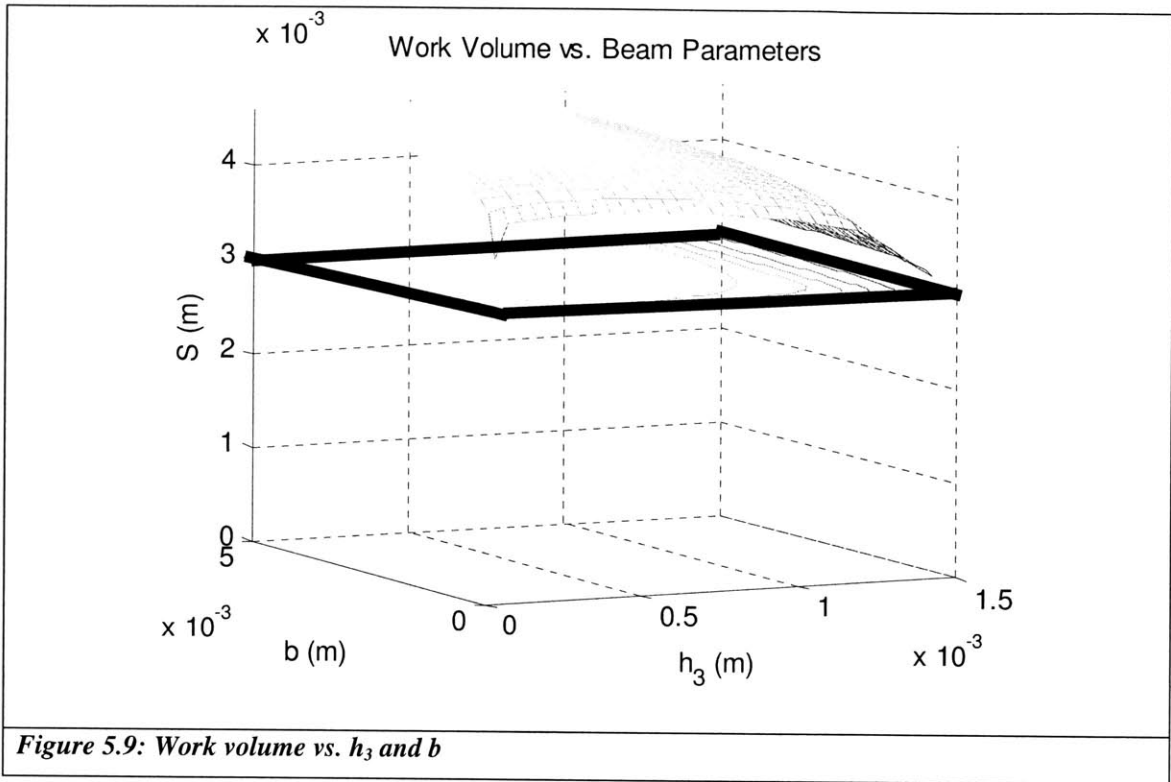
The results of the optimization are listed in Table 5.4 and Table 5.5. The optimization met all requirements.

Table 5.4: Final performance values and variation due to tolerances for the case study	
1	Transmission ratio $\approx 2 \pm 0.1$
2	Work volume $\approx 4.5mm \pm 0.5mm$
3	Energy efficiency $\approx 50\% \pm 7\%$

Table 5.5: Final parameter values for the case study optimization	
L_1	70mm
L_2	32mm
h_1	0.75mm
h_2	0.75mm
h_3	0.75mm
b	1.6mm

CHAPTER 6

6 CONCLUSIONS

6.1 Chapter overview

The purpose of this chapter is to summarize the contents of this thesis. A discussion is included

containing the hypotheses, the intellectual contribution of this work, the impact on compliant

mechanism design, how the work will be disseminated, and future work that could be done.

6.2 Review of research hypotheses

Table 6.1 summarizes the major hypotheses and describes how they were verified.

Table 6.1: Research hypotheses and how they were verified		
	Hypothesis	Verification method
1	VBMs provide a flexible means of optimizing mechanisms by not only offering a single point of operation, but an area over which the designer can choose to make design tradeoffs.	VBMs were used to optimize a single input single output mechanism and showed its robustness to manufacturing errors. The final plots demonstrated a range of values over which the mechanism's performance met specifications
2	The number of plots needed to optimize a mechanism is equal to or less than $N*P/2$	A mechanism was optimized using 7 plots, where $N*P/2$ was 9.
3	Nondimensional analysis can be used increase the density of information displayed on a visual plot of CM performance	The efficiency of a four-bar compliant mechanism was condensed from 6 parameters into one parameter on a 2-D plot in Section 4.4. This shows that if the mechanism output can be normalized to the mechanism stiffness, the efficiency of the mechanism is purely a function of that normalized value.
4	Visual-based methods are the best means of displaying large amounts of performance information	Compared VBMs to numbers, vectors, equations, and matrices – experiment by the reader confirms the ease of extracting design information using VBMs compared to looking at numbers, equations, or matrices, etc.

6.3 Intellectual contribution and impact

This thesis has presented several contributions to the field of compliant mechanism design. The main contributions are:

(1) The method of CM optimization and post-optimization validation using visual-based methods

96

(2) The discussion of the link between compliant mechanism design and user perceptions of data

(3) The nondimensional model of the compliant four-bar mechanism, which includes demonstration of how to nondimensionalize compliant beam elements and incorporate the nondimensional model into visual-based methods.

The impact of (1) is that designers now have an alternative form of optimization that provides intuitive links between mechanism parameters and performance. Knowing how each part of the mechanism contributes to the overall performance fosters better overall understanding. This method is readily applicable to concepts created using traditional mechanism synthesis techniques or constraint-based design principles. However, it is not as compatible with topological synthesis methods because the design intent of concepts is not understood by the designer. This makes it difficult to reduce and select the mechanism parameters used in optimization.

Point (2) will influence CM designers to use visual-based methods, as they efficiently present information on CM performance metrics that is not generated using standard FEA, optimization, or sensitivity analysis.

The nondimensional model discussed in (3) can serve as both a building block and a general method by which to nondimensionalize other compliant mechanisms. The nondimensional numbers taken from the model allow a denser display of performance data. Normally, plots take one variable per axis. Using a nondimensional model, all mechanism parameters can be

accounted for at once. In the case of the compliant four-bar mechanism of Chapter 4, 6 parameters were plotted on a single axis.

The practical impact of this thesis is that the visual-based methods and nondimensional models contained within can be applied to many real-world scenarios of CM design and optimization. The nondimensional model and 3-D plots give insight into the scaling relationships of parameters and how they relate to performance. This is critical in industries where for instance a complete understanding of designs is required for safety reasons, e.g. medical devices and aerospace. Future work will no doubt involve developing nondimensional models of more complex mechanisms.

In the field of optical engineering, a specific application of this research might be the design of a compliant four-bar that is used to mount an optical element. The mount would enable precise position adjustment of the optical element about a well-defined axis, i.e. instant center. Many engineers would choose to go straight to FEA for the purpose of analysis, but might have no idea where to begin choosing dimensions of the four-bar. The models developed in this thesis would enable accurate first-order analysis of the mechanism. The stiffness could be predicted using Equations 4.8 and 4.13. This could be used to find the required actuation force and resonant frequency. Equation 4.34 could be used to predict the range of motion of the mechanism. Using first-order equations, the designer would know (1) how to begin designing the optical mount and (2) how to appropriately scale dimensions to achieve desired performance. Point (1) would allow sizing of the mechanism's dimensions to within several percent of truly optimized values, and point (2) has the potential to reduce the total number of FEA iterations to two or three. This is in contrast to not using an analytical model, where the number of iterations would be governed by

the designer's ability to guess at solutions. Without knowing how performance scales with parameters, the designer may be caught in a time-consuming loop where each parameter is iterated independently in a serial fashion. If each parameter were to take five iterations on average using guesswork, the optimization of a CM with just three variable parameters could take 15 FEA iterations.

6.4 Recommendations for future work

Much work remains in the nondimensional modeling of compliant mechanisms. The main topics to be addressed are listed below:

1. Modeling efficiency to account for finite mechanism stiffness between the input and output. In the compliant four-bar model, the coupler link was considered to be infinitely rigid. The addition of compliance between the input and output affects all performance metrics of a mechanism by:

   a. Reducing the transmission ratio of the mechanism

   b. Decreasing the work volume of the mechanism

   c. Reducing the efficiency of the mechanism

   d. Decreasing the nominal stiffness of the mechanism

2. Accounting for dynamics in mechanism performance. All analysis in this thesis was quasi-static. Dynamic performance analysis is necessary especially in designing precision mechanisms.

3. A user study comparing visual-based methods to traditional optimization methods. While it has been demonstrated why, what, where, and how visual-based methods are useful, one hypothesis could be that they are "easier" to use than traditional methods. Easier in this context could be measured by the amount of time it takes someone to (1) learn the method and (2) use the method to optimize a mechanism.

4. Incorporating visual-based methods in topological synthesis of compliant mechanisms. As stated previously, topological synthesis methods exclude designers from the design loop, meaning concepts are generated without specifically indicating what intent exists in the design. Understanding of design intent is critical to understanding how to choose the parameters that describe the design. To make visual-based methods more compatible with topological synthesis methods, two approaches could be taken.

   a. Design principles could be coded into synthesis routines used by computers. The nature of design principles generally requires pattern recognition of some sort, so an undertaking of this nature may be difficult in practice. The nature of the work in part (a) would be largely fundamental research because it would require the translation and formalization of the logic of human-thought processes into symbols, equations, and functions that can be understood by a computer.

   b. A second option would be to reverse-engineer concepts and extract design intent information using constraint-based design principles. This is easier in practice than (a) because it only requires an engineer to learn these principles without requiring him or her to translate those principles into code that is understandable

by a computer. The nature of this work is more engineering than research because it involves the applications of established principles in specific cases.

5. Incorporating visual-based methods into the pseudo-rigid body model (PRBM). The PRBM has its own set of variables that it uses to approximate the behavior of compliant mechanisms. Research could be done to determine how to best select PRBM variables to display them on visual plots.

6.5 Final remarks

This thesis documents the formulation of visual-based methods in CM optimization and post-optimization validation. Visual-based methods are able to provide important design information to designers and are able to make the CM optimization process more robust. They also allow a degree of flexibility in optimization that was previously not encountered using traditional optimization methods. This flexibility enables the designer to move away from objective functions and make design tradeoffs.

A new model of a compliant beam was derived from existing models that is applicable to CM analysis using instant centers. The model can predict mechanism stiffness to within 3% of FEA results for a compliant four-bar mechanism with a well-defined instant center. This model was also used in creating nondimensional equations describing mechanism performance. The nondimensional equations were successful in producing a generalized form of mechanism performance accurate to within 5% of FEA and predicting nonlinear CM behaviors e.g. change in region of maximum stress. A case study is presented to help in interested reader through a visual-based optimization procedure.

101

This page is intentionally left blank.

REFERENCES

[1] Culpepper, ML, Anderson, G, "Design of a low-cost Nanomanipulator which utilizes a monolithic, spatial compliant mechanism", Prec Eng 2003.

[2] Diwekar, Urmila M. "Introduction to applied optimization." Norwell, Mass.: Kluwer Academic Publishers, c2003.

[3] Svanberg, Krister. "The Method of Moving Asymptotes – a New Method for Structural Optimization." Int. J for Numer. Methods in Eng.: 24, p359-373. 1987.

[4] Petri, Patrick, "A Continuum Mechanic Design Aid for Non-planar Compliant Mechanisms," Masters Thesis, MIT, Cambridge, MA, September 2002.

[5] Szczesny, Spencer, "Design of Compliant Mechanisms for Attenuation of Unidirectional Vibrations in Rotational Systems," Masters Thesis, MIT, Cambridge, MA, February 2005.

[6] Ananathasuresh, G. K. Kota, S. Gianchandani, Y. "A Methodical Approach to the Design of Compliant Micromechanisms." Solid-State Sensor and Actuator Workshop, Hilton Head, South Carolina. 189: 1994.

[7] Frecker, M. I., Ananthasuresh, G. K., Nishiwaki, S., Kikuchi, N. and Kota, S. "Topological Synthesis of Compliant Mechanisms Using Multi-Criteria Optimization." Transactions of the ASME. 119: (1997). pp. 238.

[8] Kota, Sridhar. Hetrick, Joel. Li, Zhe. Laxminarayana, Saggere. "Tailoring Unconventional Actuators Using Compliant Transmissions: Design Methods and Applications." IEEE/ASME Transactions on Mechatronics. 4, (1999): 4

[9] Sigmund, Ole. "On the Design of Compliant Mechanisms Using Topology Optimization." Mech. Struct. & Mach., 25(4) 493-524 (1997).

[10] Joo, J., Kota, S., Kikuchi, N. "Topological Synthesis of Compliant Mechanisms Using Linear Beam Elements." Mech. Struct. & Mach., 28(4) 245-280 (2000).

[11] Hetrick, J., Kikuchi, N., Kota, S., "Robustness of Compliant Mechanism Topology Optimization Formulations." SPIE Conference on Mathematics and Control in Smart Structures, Newport Beach, CA, March, 1999. pp. 244, Vol. 3667.

[12] Howell, Larry L. Compliant Mechanisms. John Wiley & Sons, Inc. New York: 2001.

[13] Maxwell, James Clerk. "General Considerations Concerning Scientific Apparatus", Scientific Papers v. 2, ed. W.D. Niven, Dover Publications, 1952.

[14] Blanding, Douglass. L. "Principles of Exact Constraint Mechanical Design" Eastman Kodak Company, Rochester, New York, 1992.

[15] Hale, Layton C. Priciples and Techniques for Designing Precision Machines. PhD Disseration, Massachusetts Institute of Technology: 1999.

[16] Suh, Nam P., The Principles of Design. Oxford University Press. New York: 1990.

[17] Erdman, Arthur G., Sandor, George N., Kota, Sridhar. Mechanism Design. Prentice Hall. Upper Saddle River, New Jersey: 2001.

[18] Lu, Kerr-Jia. Kota, Sridhar. Compliant Mechanism Synthesis for Shape-Change Applications: Preliminary Results. Procedings of the SPIE. v.4693 p.161 – 172, 2002.

[19] Lu, Kerr-Jia. Kota, Sridhar. Design of Compliant Mechanisms for Morphing Structural Shapes. Journal of Intelligent Material Systems and Structures. v.14 p.379 – 391, 2003.

[20] Lu, Kerr-Jia. Kota, Sridhar. Synthesis of Shape-Morphing Compliant Mechanisms Using Load Path Representation. Proceedings of IMECE '03. 2003.

[21] Bathe, Klaus-Jürgen. Finite Element Procedures. Prentice Hall. Upper Saddle River, New Jersey: 1996.

This page is intentionally left blank.

APPENDIX A: Optimization code – high level elements – simplemech_optimization.m

The first program contains the outer (high level) elements of the optimization algorithm and calls all of the other programs.

```
%simplemech_optimization.m
%This program was used for optimizing the mechanism in Chapter 5
%It needs no external inputs, but it requires several other functions to
%operate.

function simplemech_optimization()
close all
global KG CG beams nodes plates prop L SortRank Gr P sigmay E G;
global n N B F;
global node_tree beam_dim;
global TEES KAYS;

%Mechanism parameters (names, units, and values)
%                 1           2           3           4           5           6
dim_names={'L_1 (m)','h_1 (m)','L_2 (m)','h_2 (m)','h_3 (m)','b (m)'};
beam_dim=[    .07,    .00076,    .032,    .00076,    .00076,    .0016];

%Select the dimensions to plot (e.g. dims(1)=5 is 'h_3 (m)' from dim_names)
```

```
%Change these numbers
dims=[5 6];

%Create the mechanism and define the locations of all nodes,
%thicknesses of all beams, etc.
simple_mech(beam_dim);

%Define the input/output node numbers
ForceNode = [1];
DispNode = [3];

%Output stiffness N/m
K0=1800;

%Draw the mechanism
mechanism;

%Initialize
KG = zeros(F*6);
L=zeros(B,1);

%Define the actuator
f=zeros(n,1);
f_in=[0;1;0;0;0;0];
f(ForceNode*6-5:ForceNode*6,1)=f_in;

%Define the parameter bounds on the design plots
min1 = .0001; max1 = .0015;
min2 = .0005; max2 = .005;

% Number of steps between the min and max values of the bounds
steps = 30;
bounds1=min1:(max1-min1)/steps:max1; bounds2=min2:(max2-min2)/steps:max2;
size_b1 = size(bounds1,2);
size_b2 = size(bounds2,2);

%Initialize variables
nom_stiff=zeros(size(bounds1,2),size(bounds2,2));
eta=zeros(size(bounds1,2),size(bounds2,2));
Tr=zeros(size(bounds1,2),size(bounds2,2));
S=zeros(size(bounds1,2),size(bounds2,2));
max_stress_beam=zeros(size(bounds1,2),size(bounds2,2));
i=0; j=0; tic;

%The for loops that determine nominal stiffness, work volume, transmission
%ratio, and efficiency
for i=1:size_b1
    for j=1:size_b2
        %Assign values to the parameters, so essentially this means
        %"set this particular mechanism dimension to this particular value"
        beam_dim(dims(1))=bounds1(i);
        beam_dim(dims(2))=bounds2(j);

        %Functikon that re-create the mechanism and determine the locations
        %of all nodes, thicknesses of all beams, etc.
        simple_mech(beam_dim);
        %Function that builds the stiffness matrix, KG (a script). See
```

```
        %Reference [4]
        buildK;
        %Function that inverts the stiffness matrix to get CG, the
        %compliance matrix. See reference [4].
        InvKG();
        %Define the forces, find global displacements
        f_in=[0;1;0;0;0;0];
        f(ForceNode*6-5:ForceNode*6,1)=f_in;
        x=CG*f;
        xout=x(DispNode*6-5:DispNode*6-4);
        %Calculate the nominal stiffness at the input without the output
        %attached
        nom_stiff(j,i) = sqrt(f_in(1)^2+f_in(2)^2)/sqrt(xout(1)^2+xout(2)^2);
        %Define the output stiffness matrix
        Kout=[K0 0;0 K0];
        %Add the output stiffness matrix to the global stiffness matrix
        D=DispNode;
        KG(D*6-5:D*6-4,D*6-5:D*6-4)=KG(D*6-5:D*6-4,D*6-5:D*6-4)+Kout;
        InvKG();
        x=CG*f;
        xout=x(DispNode*6-5:DispNode*6-4);
        xin=x(ForceNode*6-5:ForceNode*6-4);
        %Calulate input and output energies and efficiency
        Eout=0.5*xout'*Kout*xout;
        Ein=0.5*x'*f;
        eta(j,i)=Eout/Ein;
        %magfinder2 is a function that implements Equation (3.2)
        [a,b]=magfinder2(f);
        S(j,i)=a*sqrt(x(DispNode*6-5)^2+x(DispNode*6-4)^2);
        max_stress_beam(j,i)=b;
        %Calculate transmission ratio
        Tr(j,i)=sqrt(xout(1)^2+xout(2)^2)/sqrt(xin(1)^2+xin(2)^2);
    end
end
time=toc


% transform the m by n array into an m times n length vector so they can
% be used in least squares error fitting to a surface
k=0;
for i=1:size_b1-1
    for j=1:size_b2-1
        k=k+1;
        linx(k,1)=bounds1(i);
        liny(k,1)=bounds2(j);
        linz1(k,1)=Tr(j,i);
        linz2(k,1)=eta(j,i);
        linz3(k,1)=S(j,i);
    end
end


% Make mesh and contour plots of all the information
figure(2)
% subplot(211)
meshc(bounds1,bounds2,Tr)
colormap(gray)
axis([0,max1,0,max2,0,matmax(Tr)]);
xlabel(dim_names(dims(1)));
```

```
ylabel(dim_names(dims(2)));
zlabel(strcat('Tr'));
title('Tr vs. Beam Parameters')
% LSEpoly(linx,liny,linz1);

figure(3)
% subplot(211)
meshc(bounds1,bounds2,eta)
colormap(gray)
axis([0,max1,0,max2,0,matmax(eta)]);
xlabel(dim_names(dims(1)));
ylabel(dim_names(dims(2)));
zlabel(strcat('\eta'));
title('Efficiency vs. Beam Parameters')
% LSEpoly(linx,liny,linz2);

figure(4)
% subplot(211)
meshc(bounds1,bounds2,S)
colormap(gray)
axis([0,max1,0,max2,0,matmax(S)]);
xlabel(dim_names(dims(1)));
ylabel(dim_names(dims(2)));
zlabel('S (m)');
title('Work Volume vs. Beam Parameters')
% LSEpoly(linx,liny,linz3);

figure(5)
% subplot(211)
meshc(bounds1,bounds2,nom_stiff)
colormap(gray)
axis([0,max1,0,max2,0,matmax(nom_stiff)]);
xlabel(dim_names(dims(1)));
ylabel(dim_names(dims(2)));
zlabel('Nominal Stiffness (N/m)');
title('Nominal Stiffness vs. Beam Parameters')
% LSEpoly(linx,liny,linz3);

figure(6)
meshc(bounds1,bounds2,max_stress_beam)
colormap(gray)
axis([0,max1,0,max2,0,matmax(max_stress_beam)]);
xlabel(dim_names(dims(1)));
ylabel(dim_names(dims(2)));
zlabel('Failing Beam');
title('Failing Beam vs. Beam Parameters')
```

APPENDIX B: Optimization code – mechanism constructor – simple_mech.m

The code in this section is used to construct a mechanism based on a set of mechanism parameters. The input is the set of mechanism parameters defined in the variable beam_dim. The variable node_tree is manually coded to capture the design intent of the concept. The output of the code is captured in the set of CoMeT variables for use in stiffness matrix analysis. These variables are: N, nodes, beams, plates, prop, L, SortRank, Gr, P, sigmay, E G, n, N, B, F [4].

```
%simple_mech.m

function simple_mech(beam_dim)
global KG CG beams nodes plates prop L SortRank Gr P sigmay E G;
global node_tree;
global n N B F;

%See Ref. 4 for a description of the variables N, nodes, beams, plates,
%prop, L, SortRank, Gr, P, sigmay, E G, n, N, B, F

N=6;
```

```
node_tree = zeros(N,7);

% node_tree contents: row # = node #
% Columns are (in this order): reference node, elevation (rad),
% azimuth (rad), distance (inches), x, y, z positions (inches)
% Here the reference nodes and relative angles are established
node_tree(1,1:7)=[4,0,-pi/2,beam_dim(1),0,0,0];
node_tree(2,1:7)=[3,0,-pi/2,.08,0,0,0];
node_tree(3,1:7)=[4,0,pi,beam_dim(3),0,0,0];
node_tree(4,1:7)=[4,0,0,0,.08,.08,0];
node_tree(5,1:7)=[2,0,pi,.08-beam_dim(3),0,0,0];
node_tree(6,1:7)=[3,0,pi,.08-beam_dim(3),0,0,0];

%The order in which the nodes positions are calculated is critical.
%The 1 more more reference nodes with fixed positions are placed first,
%and subsequent nodes are created based upon their inherited positions
node_build_order=[4 3 2 1 5 6];
% Here the actual node coordinates are established
for i=1:N
    j=node_build_order(i);
    xyz = node_tree(node_tree(j,1),5:7);
    length = node_tree(j,4);
    node_tree(j,5) = xyz(1) + length*sin(node_tree(j,3))*cos(node_tree(j,2));
    node_tree(j,6) = xyz(2) + length*cos(node_tree(j,3))*cos(node_tree(j,2));
    node_tree(j,7) = xyz(3) + length*sin(node_tree(j,2));
%       node_tree(:,5:7)
end
nodes=node_tree(:,5:7);

%Definition of other CoMeT variables
beams=[1 4;
    2 5;
    3 6;
    1 2];

P = 1;

plates=[2 3];
SortRank=[0;1;1;2;2;2];

Gr = 3;
B=size(beams,1); %number of beams
F=N-Gr;      %number of free nodes; all nodes in a free plate are considered
free.
n=F*6;       %size of K

prop=[0      0      beam_dim(2) beam_dim(6) 0      0;
0      0      beam_dim(5) beam_dim(6) 0      0;
0      0      beam_dim(5) beam_dim(6) 0      0;
0      0      beam_dim(4) beam_dim(6) 0      0];

%Mechanical properties (7075 T6 aluminum)
sigmay = 500e6;

E = 72e9;

G = 27e9;
```

APPENDIX C: Optimization code –range of motion calculator – magfinder2.m

This program returns (1) the scaling factor $\sigma_{allowable}/\sigma_{proof}$. This is used to multiply x_{proof} to find x_{max} from Equation 3.2. This program also returns the beam number which has the highest stress and is the limiting factor in the range of motion.

```
magfinder2.m

function [mag,max_stress_beam] = magfinder2(force)
global KG CG beams nodes plates prop L SortRank Gr P sigmay E G;
global n N B F;
global TEES KAYS;

x=CG*force;

for i=1:B
    %finding global displacements of beam ends
    l=L(i);
    if SortRank(beams(i,1)) < P+1
        x1=x(beams(i,1)*6-5:beams(i,1)*6,1);
        if SortRank(beams(i,2)) < P+1
            x2=x(beams(i,2)*6-5:beams(i,2)*6,1);        %1 free, 2 free
```

```
            else
                x2=zeros(6,1);                  %1 free, 2 grounded
            end
        else
            x1=zeros(6,1);
            if SortRank(beams(i,2)) < P+1
                x2=x(beams(i,2)*6-5:beams(i,2)*6,1);    %1 grounded, 2 free
            else
                x2=zeros(6,1);                  %1 grounded, 2 grounded
            end
        end
        x1=TEES(i*6-5:i*6,1:6)*x1;
        x2=TEES(i*6-5:i*6,1:6)*x2;
        Tl=[1 0 0 0 0 0;
            0 1 0 0 0 0;
            0 0 1 0 0 0;
            0 0 0 1 0 0;
            0 0 -1 0 1 0;
            0 1 0 0 0 1];
        xbeam=x2-Tl'*x1;
        fbeam=KAYS(i*12-5:i*12,7:12)*xbeam;
        %CoMeT stresses...
        Stresses(1,i)=FindMaxStress(1,prop(i,:),fbeam);
end

mag=sigmay/matmax(abs(Stresses));
Max=0;
MaxBeam=0;
for i=1:B
    ThisBeamMaxStress = max(abs(Stresses(:,i)));
    if (ThisBeamMaxStress > Max)
        MaxBeam=i;
        Max=ThisBeamMaxStress;
    end
end
max_stress_beam=MaxBeam;
```

APPENDIX D: Optimization code – displaying a mechanism in MATLAB – mechanism.m

This code draws the mechanism shown in Figure 5.1.

```
% Reconfigurable Compliant Mechanism Design Tool
% function plots the Mechanism based on the nodes, beams and plates data
contained
% in nodefile,beamfile and platefile respectively
% Modified 17th May 2005 by Kartik M. Varadarajan
% USAGE: mechanism (nodefile,beamfile,platefile)
% Modified 16th June 2005 by Richard Timm
% new feature: grounded nodes are green

% nodes = Nx3 matrix
% beams = Mx7 matrix
% P = No. of plates
% Read in beam orientation data, coordinates of point P used to determine
```

```
% ------------------------------------------------------------------

% Plot the Mechanism Geometry
figure(1)
set(gcf,'Name','Mechanism Geometry');
hold on;
xlabel('X axis');
ylabel('Y axis');
zlabel('Z axis');

% Plot beams
for (bn= 1:B)
    X = [nodes(beams(bn,1),1), nodes(beams(bn,2),1)]; % mth beams jx and kx
coordinates
    Y = [nodes(beams(bn,1),2), nodes(beams(bn,2),2)]; % mth beams jy and ky
coordinates
    Z = [nodes(beams(bn,1),3), nodes(beams(bn,2),3)]; % mth beams jz and kz
coordinates
    plot3(X,Y,Z,'-r','Linewidth',3);                   % Plot beams as red line
and node as square
end

% Plot plates
for (pn= 1:P)
    i=0;
    clear X Y Z;
    for (qn=1:size(plates,2))
        if(plates(pn,qn)~=0)
            i=i+1;
            X(i,1)=nodes(plates(pn,qn),1);
            Y(i,1)=nodes(plates(pn,qn),2);
            Z(i,1)=nodes(plates(pn,qn),3);
        end
        plot3(X,Y,Z,'-cs','Linewidth',3);              % Plot beams as cyan
line and node as square
    end
end

% Plot grounded nodes as black
X = nodes(N-Gr+1:N,1);
Y = nodes(N-Gr+1:N,2);
Z = nodes(N-Gr+1:N,3);
plot3(X,Y,Z,'ks','MarkerSize',8,'LineWidth',3);  % Plot grounded nodes as
black squares
clear X Y Z

% Plot input node as blue
X = nodes(ForceNode,1);
Y = nodes(ForceNode,2);
Z = nodes(ForceNode,3);
plot3(X,Y,Z,'g.','MarkerSize',30,'LineWidth',3);  % Plot input nodes as green
dots
clear X Y Z

% Plot output node as green
X = nodes(DispNode,1);
Y = nodes(DispNode,2);
```

```
Z = nodes(DispNode,3);
plot3(X,Y,Z,'bo','MarkerSize',8,'LineWidth',3);   % Plot output nodes as blue
circles

clear X Y Z bn pn on

% grid on;
view(2);
% axis auto;
axis equal;
hold off;
% ------------------------------------------------------------------
```

This page is intentionally left blank.